Fig. 1. Structural studies of CMESC-derived cardiomyocytes. (A) Phase contrast microscopy of the undifferentiated CMESC (left), and typical cardiomyocyte-containing non-cystic embryoid body (EB) (center). Immunofluorescent microscopy of cryosections of EBs using anti-α-Actinin and Nkx2.5 antibodies. (B) Double immunofluorescent staining for Nkx2.5 or GATA4 combined with α-Actinin, MHC, MLC, Tropomyosin or ANP. (C) Transmission electron microscopy of the CMESC-derived cardiomyocytes: striated muscle fiber (left, black arrow), desmosomal structure (middle, white arrow head) and mitochondria (right, black arrow head). Scale bars: (A) 100 μm; (B), 20 μm; (C) 0.5 μm.

Time course of marker gene expression during cardiomyocyte differentiation

To characterize the differentiation pathway of undifferentiated CMESC into cardiomyocytes, we performed semi-quantitative RT-PCR to analyze the expression of various marker genes associated with pluripotency, visceral endoderm, and early and late cardiomyogenesis. Some of the primers used have been described previously [7,10], and some were designed based on similar murine, *macaca fascicularis* and *homo sapiens* sequences (Supplementary Table 1). The pluripotency markers *Nanog* and octamer-binding transcription factor 3 (*Oct3/4*) were expressed at high levels in

undifferentiated ES cells. Expression levels of both markers gradually decreased upon differentiation and completely disappeared at day 15 post-differentiation (Fig. 2A). The early mesendoderm marker Brachyury was observed from day 3 post-differentiation, peaked at day 6 post-differentiation, but could not be detected at day 9 post-differentiation (Fig. 2B). The visceral endoderm marker alpha-fetoprotein (AFP) was observed from day 3 post-differentiation and peaked at day 9 post-differentiation, but could not be detected at day 15 post-differentiation (Fig. 2C). For the genes encoding cardiac-related transcription factors, the expression of the friend of GATA 2 (FOG-2) was first observed from day 3 post-differentiation, GATA4 and the t-box 20 (Tbx-20) were from day 6 post-differentiation, Tbx5 was from day 9 post-differentiation, and Nkx2.5 was strongly observed at day 15 post-differentiation (Fig. 2D). For the cardiomyocyte-specific proteins, ANP and the MLC 2 atrial (MLC2a) were observed first from day 6 post-differentiation, α-MHC and β-MHC were from day 9 post-differentiation, the MLC 2 ventricular (MLC2v) was from day 12 post-differentiation (Fig. 2E).

Action potential recordings of CMESC-derived cardiomyocytes

We recorded the action potentials of CMESC-derived cardiomyocytes using glass microelectrodes. Eight-week-old contracting EBs were selected manually and dispersed into small clumps and single cells. The dispersed EBs were cultured to confluence for three days before analysis. The microelectrode was advanced to the intracellular cytoplasm and the voltage of the bulk solution and cytoplasm were measured. Rhythmic beating could be detected in the CMESC-derived cardiomyocytes. The action potential resembled a sinus node, indicating that the CMESC-derived cardiomyocytes had a relatively shallow resting membrane potential, slow diastolic depolarization and relatively long action potential duration (Fig. 3A). The administration of isoproterenol increased their beating rates (Fig. 3B). The basic cycle length (BCL), action potential duration (APD), dV/dt, action potential amplitude (APA) and maximum diastolic potential (MDP) were also recorded (Fig. 3C).
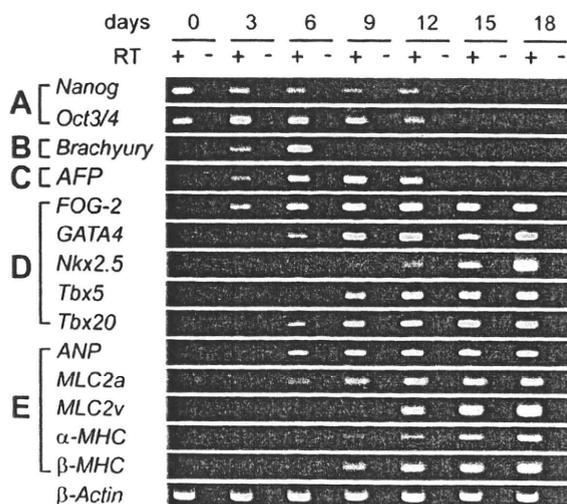

Fig. 3. Electrophysiology of CMESC-derived cardiomyocytes. (A) Representative action potentials of CMESC-derived cardiomyocytes showing spontaneous beating (left) and the relatively short duration time of the action potential (right). (B) Effect of isoproterenol (ISP) on the beating rate. (C) Statistical parameters obtained from 12 cardiomyocytes including beating cycle length (BCL), action potential duration (APD), dV/dt max, action potential amplitude (APA) and maximum diastolic potential (MDP).

Proliferative potential of CMESC-derived cardiomyocytes

Since the gestation period of the common marmoset is approximately seven times longer than that of the mouse, we hypothesized that CMESC-derived cardiomyocytes also retain their proliferative potential for a longer period of time and investigated this possibility. When EBs were dispersed into small clumps we observed a relatively long-term proliferation period and noticeable cell multiplication. From these findings, we expected that CMESC-derived cardiomyocytes might possess a higher proliferation ability than mouse-derived ES cells.

First, we performed BrdU incorporation assays on intact EBs at several time points after differentiation had occurred. The identification of DNA synthesizing cardiomyocytes was confirmed by co-immunofluorescent staining of Nkx2.5 and BrdU. At 6 weeks, intact EBs initially contained 33% BrdU-positive cardiomyocytes, but this decreased to less than 1% at 12 weeks (Fig. 4A and B). Next, the dispersed cells from EBs at several time points were applied to BrdU incorporation assays. Average 73% of cardiomyocytes were positive for BrdU at 5 weeks. This gradually decreased to 30% at 24 weeks, and 0% at 36 weeks (Fig. 4A and C). Most of the cardiomyocytes from freshly dispersed EBs 36 weeks after differentiation were rod-shaped (data not shown). These data indicated that common marmoset ES cell-derived cardiomyocytes retained their proliferation potential for an extended period of time.

Discussion

This is the first study to demonstrate that CMESC can differentiate into cardiomyocytes *in vitro*. We described their overall differentiation mechanism including time-courses for the expression of various genes during cardiogenesis, and characterized them in

Fig. 2. RT-PCR analysis of the CMESC-derived EBs for various immature and cardiomyocyte-specific proteins. (A) Pluripotency-related genes: Nanog and Oct3/4; (B) Mesodermal marker gene: Brachyury; (C) Primitive endodermal marker gene: AFP; (D) cardiomyocyte-precursor and cardiomyocyte marker genes: FOG-2, GATA4, Nkx2.5, Tbx5, and Tbx20; (E) Cardiomyocyte-associated structural protein genes: ANP, MLC2a, MLC2v, α-MHC, β-MHC, and equal loading control β-actin. Reverse-transcription negative controls were also amplified and loaded in the lane next to the relevant sample. Abbreviations are listed in Supplementary Table 1.
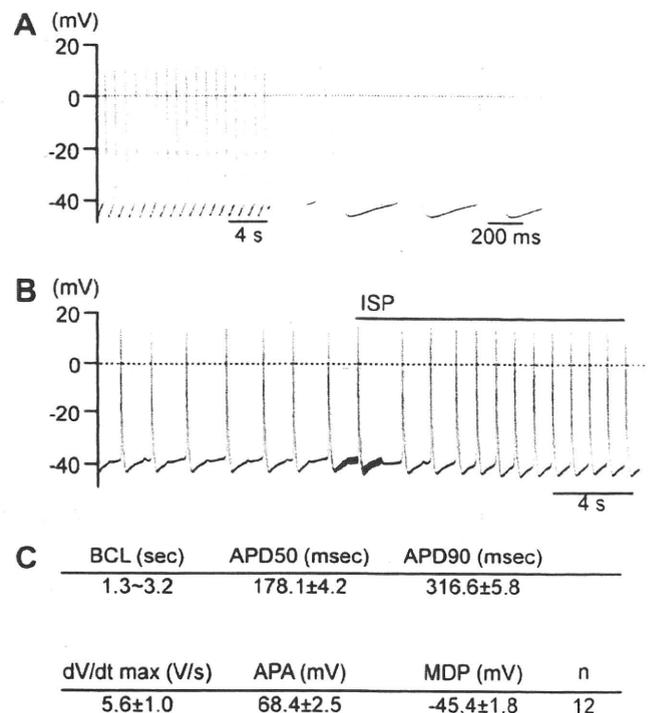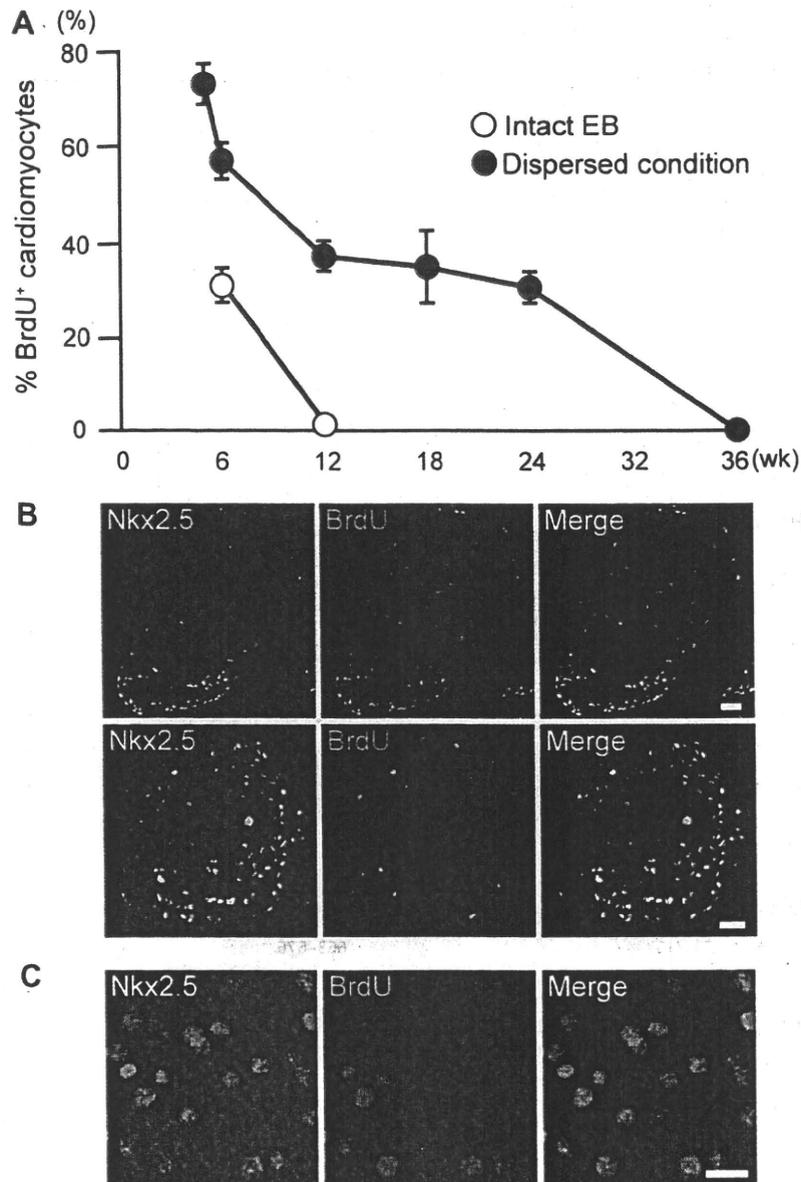
Fig. 4. Proliferation properties of CMESC-derived cardiomyocytes. (A) Time course BrdU incorporation assay in intact EB (open circle; $n = 3$) and dispersed condition (closed circle; $n = 3$) during weeks 5–36 post-differentiation. Cardiomyocytes were identified by immunofluorescent staining for Nkx2.5. The fractions of BrdU-positive cardiomyocytes were plotted. (B) Typical immunofluorescent staining patterns of Nkx2.5 (left), BrdU (middle) and merged images (right) in the intact EBs 6 weeks after differentiation (upper panel) and 12 weeks after differentiation (lower panel). (C) Typical immunodetection of Nkx2.5 (left), BrdU (middle) and merged images (right) in the dispersed condition 6 weeks after differentiation. Scale bars: (B) 100 μm; (C) 20 μm.

detail by immunofluorescent staining, ultrastructural analysis, electrophysiology and determining their growth properties.

Gene expression analyses during cardiogenesis in several species including mice [12], humans [13], and rhesus monkeys [10] are available. The present study enabled us to obtain gene expression data for the common marmoset monkey. A comparison of gene expression profiles between the species listed above highlights many similarities. The only major difference seems be in the timing of cardiomyocyte development: 8–14 days in humans; 12 days in the common marmoset; 8 days in the rhesus monkey; and 6 days in mice. Although minor differences in the expression timings of the *ANP*, *MLC-2a*, *MLC-2v* and *α-MHC* genes also exist during differentiation, we found that the timing of CMESCs was closest to human ES cells.

We found that the efficiency of cardiac differentiation was the same when obtained under non-serum conditions using KSR instead of FCS. These observations indicated that CMESCs, unlike hu-

man [14] or rhesus monkey [10] ES cells, do not require any serum-derived stimulating factors for mesendoderm induction and cardiogenesis, because KSR does not contain any cytokines or growth factors. On the other hand, the expression of various marker genes during cardiogenesis was very similar to that seen in human [14] and rhesus monkey [10] ES cells, suggesting that CMESCs have a similar cardiogenic differentiation system to human and rhesus monkey ES cells. CMESCs might be able to provide differentiation-inducing auto- and/or paracrine factors. Further mechanistic comparative studies between CMESCs and human and/or rhesus monkey ES cells will provide further insights into cardiogenic differentiation.

BrdU incorporation assay indicated that CMESC-derived cardiomyocytes were capable of long-term proliferation for extended periods of time. Importantly, CMESC-derived cardiomyocytes were still able to proliferate 24 weeks after differentiation, but the ability to proliferate ended at 36 weeks. Considering the gestation

period of the common marmoset, these findings had a reasonable explanation.

Much information about human ES cells and their application to heart regeneration therapy has accumulated [15,16]. Moreover, mouse and human inducible pluripotent stem cells (iPS cell) have also been established [17]. In order for heart regeneration therapy using regenerated cardiomyocytes to become a reality, preclinical studies using primate ES cell- or iPS cell-derived cardiomyocytes for transplantation are necessary. The common marmoset monkey is an ideal primate model for preclinical studies in the field of regenerative medicine. We believe that this report provides fundamental details about CMESC-derived cardiomyocytes that will aid their use as a primate heart cell-therapy model.

Appendix A. Supplementary data

Supplementary data associated with this article can be found, in the online version, at doi:10.1016/j.bbrc.2008.02.141.

References

[1] W.R. MacLellan, M.D. Schneider, Genetic dissection of cardiac growth control pathways, Annu. Rev. Physiol. 62 (2000) 289–319.
[2] B. Dawn, A.B. Stein, K. Urbanek, M. Rota, B. Whang, R. Rastaldo, D. Torella, X.L. Tang, A. Rezazadeh, J. Kajstura, A. Leri, G. Hunt, J. Varma, S.D. Prabhu, P. Anversa, R. Bolli, Cardiac stem cells delivered intravascularly traverse the vessel barrier, regenerate infarcted myocardium, and improve cardiac function, Proc. Natl. Acad. Sci. USA 102 (2005) 3766–3771.
[3] K.L. Laugwitz, A. Moretti, J. Lam, P. Gruber, Y. Chen, S. Woodard, L.Z. Lin, C.L. Cai, M.M. Lu, M. Reth, O. Platoshyn, J.X. Yuan, S. Evans, K.R. Chien, Postnatal isl1+ cardioblasts enter fully differentiated cardiomyocyte lineages, Nature 433 (2005) 647–653.
[4] H. Oh, S.B. Bradfute, T.D. Gallardo, T. Nakamura, V. Gaussin, Y. Mishina, J. Pocius, L.H. Michael, R.R. Behringer, D.J. Garry, M.L. Entman, M.D. Schneider, Cardiac progenitor cells from adult myocardium: homing, differentiation, and fusion after infarction, Proc. Natl. Acad. Sci. USA 100 (2003) 12313–12318.
[5] S. Lyngbaek, M. Schneider, J.L. Hansen, S.P. Sheikh, Cardiac regeneration by resident stem and progenitor cells in the adult heart, Basic Res. Cardiol. 102 (2007) 101–114.
[6] I. Kehat, D. Kenyagin-Karsenti, M. Snir, H. Segev, M. Amit, A. Gepstein, E. Livne, O. Binah, J. Itskovitz-Eldor, L. Gepstein, Human embryonic stem cells can differentiate into myocytes with structural and functional properties of cardiomyocytes, J. Clin. Invest. 108 (2001) 407–414.
[7] E. Sasaki, K. Hanazawa, R. Kurita, A. Akatsuka, T. Yoshizaki, H. Ishii, Y. Tanioka, Y. Ohnishi, H. Suemizu, A. Sugawara, N. Tamaoki, K. Izawa, Y. Nakazaki, H. Hamada, H. Suemori, S. Asano, N. Nakatsuji, H. Okano, K. Tani, Establishment of novel embryonic stem cell lines derived from the common marmoset (Callithrix jacchus), Stem Cells 23 (2005) 1304–1313.
[8] J.A. Thomson, J. Kalishman, T.G. Golos, M. Durning, C.P. Harris, R.A. Becker, J.P. Hearn, Isolation of a primate embryonic stem cell line, Proc. Natl. Acad. Sci. USA 92 (1995) 7844–7848.
[9] H. Suemori, T. Tada, R. Torii, Y. Hosoi, K. Kobayashi, H. Imahie, Y. Kondo, A. Iritani, N. Nakatsuji, Establishment of embryonic stem cell lines from cynomolgus monkey blastocysts produced by IVF or ICSI, Dev. Dyn. 222 (2001) 273–279.
[10] K. Schwanke, S. Wunderlich, M. Reppel, M.E. Winkler, M. Matzkies, S. Groos, J. Itskovitz-Eldor, A.R. Simon, J. Hescheler, A. Haverich, U. Martin, Generation and characterization of functional cardiomyocytes from rhesus monkey embryonic stem cells, Stem Cells 24 (2006) 1423–1432.
[11] M. Hosseinkhani, K. Hasegawa, K. Ono, T. Kawamura, T. Takaya, T. Morimoto, H. Wada, A. Shimatsu, S.G. Prat, H. Suemori, N. Nakatsuji, T. Kita, Trichostatin A induces myocardial differentiation of monkey ES cells, Biochem. Biophys. Res. Commun. 356 (2007) 386–391.
[12] K.R. Boheler, J. Czyz, D. Tweedie, H.T. Yang, S.V. Anisimov, A.M. Wobus, Differentiation of pluripotent embryonic stem cells into cardiomyocytes, Circ. Res. 91 (2002) 189–201.
[13] A. Beqqali, J. Kloots, D. Ward-van Oostwaard, C. Mummery, R. Passier, Genome-wide transcriptional profiling of human embryonic stem cells differentiating to cardiomyocytes, Stem Cells 24 (2006) 1956–1967.
[14] E. Bettiol, L. Sartiani, L. Chicha, K.H. Krause, E. Cerbai, M.E. Jaconi, Fetal bovine serum enables cardiac differentiation of human embryonic stem cells, Differentiation 75 (2007) 669–681.
[15] O. Caspi, I. Huber, I. Kehat, M. Habib, G. Arbel, A. Gepstein, L. Yankelson, D. Aronson, R. Beyar, L. Gepstein, Transplantation of human embryonic stem cell-derived cardiomyocytes improves myocardial performance in infarcted rat hearts, J. Am. Coll. Cardiol. 50 (2007) 1884–1893.
[16] M.A. Laflamme, K.Y. Chen, A.V. Naumova, V. Muskheli, J.A. Fugate, S.K. Dupras, H. Reinecke, C. Xu, M. Hassanipour, S. Police, C. O'Sullivan, L. Collins, Y. Chen, E. Minami, E.A. Gill, S. Ueno, C. Yuan, J. Gold, C.E. Murry, Cardiomyocytes derived from human embryonic stem cells in pro-survival factors enhance function of infarcted rat hearts, Nat. Biotechnol. 25 (2007) 1015–1024.
[17] K. Takahashi, S. Yamanaka, Induction of pluripotent stem cells from mouse embryonic and adult fibroblast cultures by defined factors, Cell 126 (2006) 663–676.

EXPERT REVIEWS

Recent advances in cardiovascular regenerative medicine: the induced pluripotent stem cell era

Shinsuke Yuasa and Keiichi Fukuda[†]

[†]Author for correspondence
Department of Regenerative Medicine and Advanced Cardiac Therapeutics, Keio University School of Medicine, 35 Shinanomachi, Shinjuku, Tokyo 160-8582, Japan
Tel.: +81 353 633 874
Fax: +81 353 633 875
kfukuda@sc.itc.keio.ac.jp

Induced pluripotent stem (iPS) cells have recently been established by transfecting mouse and human fibroblasts with the transcription factors Oct3/4, Sox2, Klf4 and c-Myc, known to be expressed at high levels in embryonic stem (ES) cells. These cells have great potential in regenerative medicine as they have the capacity to differentiate into all three germ layer-derived cells and are syngeneic. The differentiation of ES cells into cardiomyocytes mimics the early processes involved in heart development. Recent studies describe the contribution of various growth factors and corresponding inhibitors to heart development during embryogenesis. Bone morphogenetic proteins, Wnt protein and Notch signals play critical roles in heart development in a context- and time-dependent manner. Consistent with ES cells, the exposure of iPS cells to such growth factors is hypothesized to augment differentiation into cardiomyocytes. The combination of iPS cells and appropriate developmental signal information has the potential for providing the foundations for future regenerative medicine.

Cardiovascular regenerative medicine is progressing due to the focus of many groups, including ours, on investigating the mechanisms underlying cardiomyocyte differentiation [1,2]. Although significant progress had been achieved, there is no efficient method for generating cardiomyocytes from patients. Among the many target diseases for regenerative medicine, heart disease is one of the most important therapeutic targets, owing to the high morbidity and mortality rates of heart failure. Heart failure is the outcome of many cardiac diseases, including ischemic heart disease, valvular heart disease, congenital heart disease and cardiomyopathies (dilatated, hypertrophic and restrictive cardiomyopathy). The replacement of diseased heart tissue with healthy cardiomyocytes by cell transplantation requires a potent stem cell with strong proliferation capacity and reliable differentiation ability. Although embryonic stem (ES) cells are pluripotent with strong proliferative capacity, ethical considerations make us hesitate in the establishment of new human ES cells as we

have to destroy early human embryos for the generation of human ES cells, and ES cells do not display the autologous genotype of patients [3]. To avoid these problems and to maintain stem cell characteristics, many studies have focused on cell fusion and somatic nuclear transplantation but have not progressed to successful clinical application [4,5]. The generation of murine induced pluripotent stem (iPS) cells in 2006 and human iPS cells in 2007 has provided an alternative approach to ES cells [6–8]. Human iPS cells provide a suitable system for application to cardiovascular regenerative medicine.

iPS cell generation

First, Takahashi et al. reported that mouse iPS cells are generated from adult fibroblasts by gene transfer of the transcription factors Oct3/4, Sox2, c-Myc and Klf4 [7]. After 1 year, Yanamanaka and Thomson's groups reported that human iPS cells are also established from human somatic cells by four-gene transfer of Oct3/4, Sox2, c-Myc and Klf4, or Oct3/4,

 122 **803**

Sox2, Nanog and Lin28 [6,8,9]. The morphology, growth characteristics and pluripotency of iPS cells is similar to those of ES cells. Moreover, germ-line competency of iPS cells is demonstrated using the *cis* element of Nanog as a selection marker [10]. Among the introduced transcription factors, there is a risk of tumorigenicity by reactivation of the oncogene c-Myc. iPS cells have been generated from mouse and human fibroblasts without c-Myc and these cells do not develop tumors [11]. After successful establishment of iPS cells, many researchers attempted to clarify the precise characteristics of iPS cells compared with ES cells. As genetic and epigenetic abnormalities result in multiple pathogeneses, the genetic and epigenetic status of iPS cells is intensely investigated. Global gene expression patterns are similar, but not identical, between iPS cells and ES cells in mouse and human studies [6,7,9,12]. Accumulating evidence showed that epigenetic status of iPS cells is highly similar to that of ES cells in a view of stem cell marker promoter methylation status, dynamics of X inactivation in female iPS cells and global patterning of histone methylation [6,7,9,10,13,14]. Mouse and human iPS cells also differentiate into cardiac myocytes *in vitro* and *in vivo*, similar to ES cells [6,7,13,15].

Many advantages of iPS cell have been pointed out. Successful reprogramming of differentiated human somatic cells into a pluripotent state would allow the creation of patient- and disease-specific stem cells.

- For transplantation therapies using stem cells, patient-specific iPS cells can eliminate the concern of immune rejection;
- The similarities between iPS cells and ES cells have allowed current accumulating methods for differentiation of ES cells to be adapted for the differentiation of iPS cells into cardiomyocytes for clinical use [16];
- For drug discovery, human iPS cells should make it easier to generate panels of cell lines that more closely reflect the genetic diversity of a population.

As there are many genetic disorders in the heart, such as familial dilated cardiomyopathy, familiar arrhythmia and congenital heart diseases, we need to examine development, pathogenesis and physiologic characteristics of the hereditarily diseased human cardiac myocyte. This is one of the potent merits of using iPS cells, as it is difficult to obtain many living diseased cardiomyocytes from patients for the drug screening and for several analyses.

However, it is important to understand that before the cells can be used in the clinic, further extensive work is required to determine whether human iPS cells are fully safe for clinical usage and human iPS cell-derived cardiomyocytes are truly identical with normal cardiomyocytes.

ES cells

Mouse ES cells were first established by Evans *et al.* in 1981, and the proliferative capacity and pluripotency of these cells led to the establishment of early developmental model systems and the generation of genetically modified mice, including knockout mice [3]. When implanted under the skin *in vivo*, ES cells readily form teratoma. They can differentiate into a variety of tissues in cell culture dishes in the absence of differentiation inhibitors, such as leukemia inhibitory factor or mouse embryonic fibroblast. In the mid-1990s, ES cell research slowly progressed to the use of experimental animals as *in vivo* models for cell-transplantation therapy [2]. Human ES cells were established by Thomson *et al.* in 1998 and rapidly attracted attention as a source of cells for regenerative therapy [17]. The development of ES cells for regeneration therapy has two main disadvantages. First, ethical considerations make us hesitate in the generation of new human ES cells as they are derived from preimplantation human embryos [3]. Second, ES cells do not show the autologous genotype of patients. To maintain stem cell characteristics and to avoid ethical issues many studies focused on cell fusion and somatic nuclear transplantation that succeeded at a preliminary level in animal experiments [4,5,18]. These findings raised the advantage of using somatic cells from patients to produce unique ES cell lines. Subsequent research focused on investigating the mechanisms underlying the control of ES cell differentiation to allow establishment of cell-replacement therapy. Many problems for the clinical application of such technology remain unsolved.

Differentiation of cardiomyocytes from ES cells

The differentiation of mouse ES cells into cardiomyocytes *in vitro* was first demonstrated in 1985 and it was established that such differentiation occurred at a constant rate as in other cell types [19]. Research into the use of ES cells in cell replacement therapy was initiated after the mid-1990s. In 1996, Field *et al.* reported that the stable transfection of ES cells with the aminoglycoside phosphotransferase gene under the control of the α-cardiac myosin heavy chain promoter succeeded in purifying cardiomyocytes after differentiation *in vitro* [20]. This study provided the impetus for the use of ES cells in the clinical setting. The development of methods for differentiating ES cells into cardiomyocytes more selectively and efficiently using a variety of factors progressed steadily in the late 1990s [21].

Many methods for the differentiation of ES cells into cardiomyocytes are reported. The differentiation of ES cells mimics normal embryonic development thereby providing essential information on developmental processes, including heart development. It is generally accepted that the humoral factors essential for cardiomyogenesis *in vivo* would stimulate ES cells to differentiate into cardiomyocytes *in vitro*. Information from genetically modified mice displaying cardiac abnormalities has provided information on essential factors in embryonic heart development. Cardiac anomalies occur in mice lacking the receptor for retinoic acid (RA) – a vitamin A derivative – or when vitamin A is deficient during development, implicating this factor in cardiac differentiation and development [22–24]. Furthermore, RA induces the differentiation of cardiomyocytes

123

from embryonal carcinoma cells *in vitro*, in a time- and concentration-dependent manner consistent with normal development [25]. Based on these findings, Wobus *et al.* succeeded in increasing the efficiency of cardiomyocyte induction by exposing ES cells to RA under strictly controlled conditions with respect to concentration and timing [26]. This study also showed that the differential induction of ventricular muscle was greater than other cardiomyocyte populations [26]. A later study demonstrated expression of nitric oxide (NO) synthase in the heart during mouse development and the promotion of cardiomyocyte development by NO, which thereby led to the use of NO donors or inhibitors for the differentiation of ES cells into cardiomyocytes [27]. Takahashi *et al.* screened various compounds and showed that ascorbic acid promotes the induction of cardiomyocyte differentiation [28]. Studies on the differentiation of ES cells into cardiomyocytes using known growth factors and chemical compounds are reviewed by Boheler *et al.*, Sachinidis *et al.* and Heng *et al.* [29–31].

The differentiation of ES cells into any cell lineage partly depends on the regulatory mechanisms underlying normal early development. Although several signaling proteins, including bone morphogenetic proteins (BMPs) [32–35], Wnts [36–38], Notch [39,40] and FGFs [41] are involved in heart development, little is known on the exact regulatory signals that mediate the differentiation of ES cells into cardiomyocytes. In mouse embryos, cardiac progenitor cells appear at embryonic day (E) 7.0, and the cardiac crescent is formed by E7.5, indicating that the growth factors expressed in these regions or in surrounding areas at the relevant developmental stage would be important for efficient cardiomyocyte induction.

Bone morphogenetic protein signal

The BMP family is the largest subfamily of the TGF-β superfamily. During embryonic development, specific BMPs are expressed prior to cardioblast formation and during heart organogenesis from the epiblast stage, and are involved in a broad range of developmental events including cell proliferation, differentiation, migration and apoptosis during progression of development [42–45]. At least six BMPs (BMP-2, -4, -5, -6, -7 and -10) are expressed in the heart and have independent and redundant functions [46–49]. Experiments on genetically modified mice demonstrate the importance of BMP signaling in heart morphogenesis after the mid-gestational stage. BMPs are expressed in the lateral plate mesoderm, including the anterior lateral plate (cardiogenic mesoderm), and the essential role of these signaling factors is demonstrated by the appearance of heart defects in early-stage embryos as a result of gene targeting of BMP-2 [33,47]. Application of BMP-2-soaked beads *in vivo* induces the ectopic expression of cardiac transcription factors, and the administration of soluble BMP-2 or -4 to explant cultures induces full cardiac differentiation in chick stage 5–7 anterior medial mesoderm, which would not normally be cardiogenic [50]. A BMP positive role was also shown using pluripotent mouse embryonic

carcinoma cells (P19CL6), which were able to differentiate into cardiac myocyte *in vitro* [51,52]. Noggin, a potent BMP antagonist, which was stably transfected into P19CL6, inhibited differentiation into cardiac myocyte; BMP signal downstream molecules salvaged their cardiac differentiation. However, there is a report that BMP-2 and -4 suppress cardiomyocyte differentiation in early-stage chick embryo explants, which suggests that BMPs inhibit cardiomyocyte development before and around gastrulation [53]. Together, these findings show that BMPs play a critical and dynamic role in the induction of cardiomyocytes in heart development. In the vertebrate nervous system, Noggin and other BMP inhibitors (Chordin and Follistatin) are involved in neural differentiation and patterning during embryonic development and in adult neurogenesis in a context-dependent fashion [54,55]. We showed that the BMP antagonist Noggin was expressed transiently at high levels in the heart-forming area in whole-mount *in situ* hybridization and promoted the cardiac differentiation from mouse ES cells [1]. This expression pattern was also observed in early embryos of chick and *Xenopus*, suggesting a conserved mechanism in heart development [56,57]. Based on analogy to the CNS, the context-dependent differential action of BMPs in cardiomyocyte induction may be explained by the local action of Noggin and other BMP inhibitors. Our recent report also showed that short-term BMP treatment and BMP inhibition by Noggin promoted cardiac myocyte differentiation from human ES cells and long-term BMP treatment resulted in trophoblast differentiation [58]. There are many reports in which BMPs and other TGFβ family proteins had a strong positive role in cardiac myocyte differentiation from ES cells, and BMPs certainly have a positive role in cardiomyocyte differentiation [59–61]. Taken together, the temporal and spatial regulation of BMPs and BMP antagonists reveal a critical involvement in the differentiation of cardiomyocytes during heart development.

Wnt signal

Similar to BMP signaling, the Wnt signaling pathway also has an important role in tissue development. The Wnt pathway regulates cell adhesion, morphology, proliferation, migration and structural remodeling [62–64]. The major components of this network are the Wnt ligands, which bind to Frizzled receptors at the cell surface. The Wnt ligands comprise over 17 members, with some activating the canonical pathway and others activating the noncanonical pathway [65]. In the canonical Wnt pathway, activation of Wnt signaling downregulates the intracellular degradation of β-catenin, allowing translocation to the nucleus and transcription factor activation in conjunction with the cotranscription factors Lefs and Tcfs. The noncanonical Wnt pathway has no role in β-catenin degradation but can activate c-Jun N-terminal kinase (JNK) and other signaling pathways. Wnt signaling was initially implicated as an inhibitor of cardiomyocyte induction [36–38]. The Wnt inhibitors Crescent and Dkk-1 are expressed in the anterior endoderm during chick
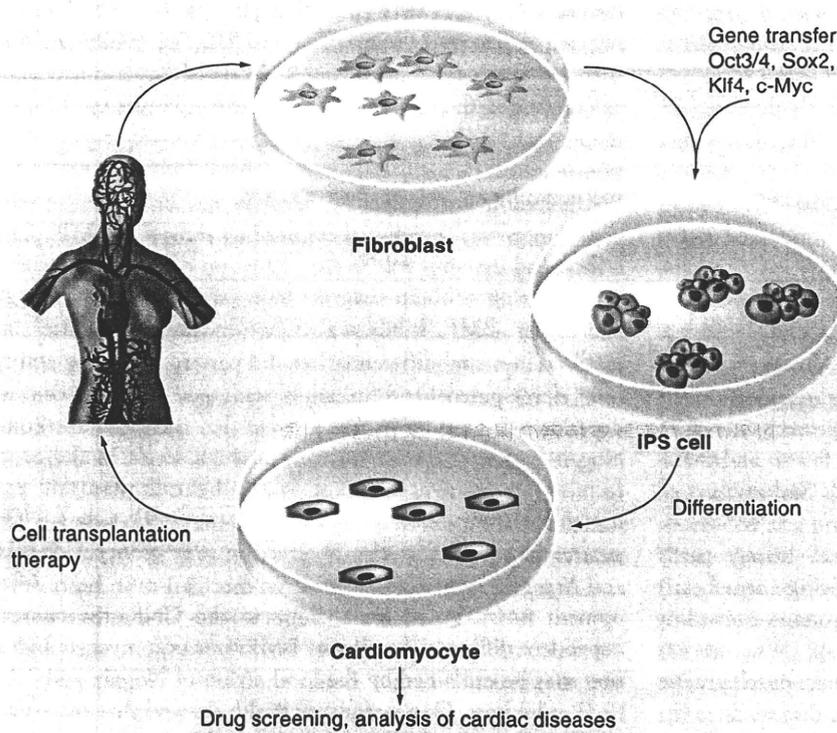
Figure 1. Cardiac regenerative medicine using iPS cells. Human fibroblasts are obtained from adult tissues. Human fibroblasts dedifferentiate into iPS cells by gene transfer. Cardiomyocytes were differentiated from iPS cells. iPS cell-derived cardiac myocytes were used for cell transplantation therapy, drug screening and analysis of cardiac diseases. iPS: Induced pluripotent stem.

gastrulation and induce formation of beating heart muscle, while ectopic Wnt signals repress heart formation from anterior mesoderm *in vitro* and *in vivo* [36,66]. The forced expression of either Wnt3A or Wnt8, known canonical Wnt pathway stimulators, promotes the development of primitive erythrocytes from the precardiac region. These findings suggest that inhibition of Wnt signaling by Dkk-1 and Crescent promotes heart formation in the anterior lateral mesoderm, whereas active Wnt signaling in the posterior lateral mesoderm promotes blood development.

In recent contrasting reports, Wnt members promote the differentiation of cardiomyocyte from ES cells. In the chick embryo, Wnt11 is expressed in the early mesoderm in a pattern overlapping with the precardiac regions and exogenous Wnt11 can promote cardiac differentiation in noncardiogenic tissue [67,68]. Subsequent loss- and gain-of-function experiments reveal that Wnt11 is required for heart formation in *Xenopus* embryos and is sufficient to induce a contractile phenotype in embryonic explants via noncanonical Wnt signaling, which involves protein kinase C and JNK [69]. Treatment of the mouse embryonic carcinoma stem cell line P19 with murine Wnt11 triggers cardiogenesis, suggesting that the function of Wnt11 in heart development is conserved in higher vertebrates [69]. Exogenous Wnt11 also promotes

the differentiation of murine ES cells into cardiomyocytes [70]. Together, these results indicate that cardiac development requires noncanonical Wnt signal transduction.

Involvement of the canonical Wnt pathway in mammalian cardiac myogenesis was examined by inducing the differentiation of P19CL6 into spontaneous beating cardiomyocytes with 1% dimethylsulfoxide (DMSO) [25,71]. DMSO induces the expression of Wnt3A and Wnt8A in the P19CL6 cells, which subsequently activates Wnt/β-catenin signaling and thereby induces cardiac myogenesis [71]. The Wnt antagonist – secreted frizzled-related protein (SFRP) – inhibited early stages of cardiomyogenesis from P19CL6 by Wnt3 transcription regulation in a stage-specific manner, preventing mesoderm specification and maintaining the cells in the undifferentiated state [72]. Evidence for the requirement of canonical Wnt signaling in heart development *in vivo* was provided by investigations of β-catenin conditional heart specific null mice [73,74]. Investigations into ES cell differentiation revealed that Sox17 regulated by canonical Wnt pathway is essential for the specification of cardiac mesoderm and a biphasic effect of canonical Wnt signaling on cardiomyocyte development [75–77]. Activation of the canonical Wnt signaling pathway in the early phase during embryoid body (EB) formation enhances the differentiation of ES cells into cardiomyocytes. By comparison, activation of the canonical Wnt pathway in the late phase after EB formation inhibits the differentiation of ES cells into cardiomyocytes [76]. The nuclear protein Chibby inhibits β-catenin signaling and has a key role in forming cardiomyocytes from ES cells after the onset of Brachyury-positive mesendoderm progenitors [78]. These findings suggest that Wnt/β-catenin signaling is activated at the inception of mammalian cardiac myogenesis and is indispensable for cardiac differentiation *in vitro* and *in vivo*.

Notch pathway

The Notch pathway is involved in differentiation and lineage decisions in fetal and postnatal development and in self-renewing organs [79,80]. The transmembrane Notch receptor is activated at the cell surface by members of the Jagged and Delta ligand families. There are four types of mouse and human Notch receptor (Notch1–4) and five ligands (Jagged1, Jagged2, Delta-like-1, Delta-like-3 and Delta-like-4) [81,82]. Notch signaling is transmitted through ligand-receptor interactions from neighboring cells. After activation, the receptor undergoes proteolytic cleavage by γ-secretase, releasing the Notch intracellular domain, which in

turn translocates into the nucleus and trimerizes with the transcription-factor recombination signal sequence binding protein (RBP)-J-κ to convert it from a transcriptional repressor to an activator [83]. The lack of RBP-J-κ expression in ES cells enhances cardiomyogenesis, whereas expression of RBP-J-κ in RBP-J-κ deficient ES cells restores repression of the cardiogenic pathway [83]. Differentiation of ES cells into cardiomyocytes is also favored by inactivation of the Notch1 receptor, whereas endogenous Notch signaling promotes differentiation of ES cells into the neuronal lineage [84]. These findings suggest that Notch signaling via RBP-J-κ is a negative regulator of cardiomyocyte induction. Subsequent studies have shown that Notch signaling is essential for cardiac development [85–87]. Further characterization of Notch signaling in cardiac development is required to progress the potential of cardiac regenerative medicine (FIGURE 1).

Conclusions

During development of the many organ systems, there is no single growth factor that acts throughout the entire process of induction. Individual factors, such as BMP, Wnt and Notch, can exert opposite actions in different developmental processes [88,89]. The in-context use of growth factor combinations will allow the specific differentiation of cardiomyocytes from ES cells. In 2001, human ES cells were induced to differentiate into cardiomyocytes with cardiac-specific structural and functional properties [90]. The same group revealed that transplanted human ES cell–derived cardiomyocytes can act as a pacemaker in porcine ventricles in which a complete atrioventricular block was artificially generated [91]. In this study, human ES cell-derived cardiomyocytes made successful electrical connections with recipient cardiomyocytes. These studies demonstrate that research into the use of ES cells for regenerative medicine has progressed rapidly in recent years. Further development of iPS cell technology will allow the knowledge gained from ES cell studies to be applied to regenerative cardiovascular medicine.

Expert commentary

Cardiac regenerative medicine is one of the most fascinating areas of clinical medicine. Bone marrow stem cells (hematopoietic stem cells and mesenchymal stem cells), skeletal muscle stem cells, endothelial progenitor cells, adipose tissue-derived stem cells and cardiac resident stem cells have been investigated for potential in regenerative medicine. In clinical trials, bone marrow stem cells were successful in preventing remodeling after acute myocardial infarction [92,93]. But in other trials, bone marrow stem cells failed to show significant benefits [94]. Ongoing trials are investigating the potential for bone marrow stem cells in regenerative medicine. ES cell and iPS cells have great potential in regenerative medicine. Investigations are focusing on understanding the mechanisms underlying the control of differentiation of these cells, including the establishment of techniques using several factors in combination to mimic *in vivo* heart development.

Five-year view

In the near and foreseeable future, cardiomyocyte regenerative medicine will be applied clinically. The advent of iPS cell technology has the potential of overcoming many of the technical problems and issues facing traditional ES cell technology. It is expected that problems in the generation of human iPS cells will be solved in the near future allowing the safe and successful application of iPS cell technology in the clinical setting.

Key issues

- The main challenge for regenerative medicine is establishment of the technology for induced pluripotent stem cells which parallels that already established for embryonic stem cells.
- The most critical technical problem is the establishment of a reliable method for the differentiation of cardiomyocytes from induced pluripotent stem cells.
- The reliable and efficient transplantation of cultured cardiomyocytes into the diseased heart is also an important issue to address as the survival of cardiomyocytes varies according to transplantation strategy.

References

Papers of special note have been highlighted as:
- of interest
- of considerable interest

1 Yuasa S, Itabashi Y, Koshimizu U *et al.* Transient inhibition of BMP signaling by Noggin induces cardiomyocyte differentiation of mouse embryonic stem cells. *Nat. Biotech.* 23(5), 607–611 (2005).

2 Fukuda K, Yuasa S. Stem cells as a source of regenerative cardiomyocytes. *Circ. Res.* 98(8), 1002–1013 (2006).

3 Evans MJ, Kaufman MH. Establishment in culture of pluripotential cells from mouse embryos. *Nature* 292(5819), 154–156 (1981).

•• Initial report that showed the establishment of embryonic stem cells.

4 Cowan CA, Atienza J, Melton DA, Eggan K. Nuclear reprogramming of somatic cells after fusion with human embryonic stem cells. *Science* 309(5739), 1369–1373 (2005).

5 Wilmut I, Schnieke AE, McWhir J, Kind AJ, Campbell KHS. Viable offspring derived from fetal and adult mammalian cells. *Nature* 385(6619), 810–813 (1997).

6 Takahashi K, Tanabe K, Ohnuki M *et al.* Induction of pluripotent stem cells from adult human fibroblasts by defined factors. *Cell* 131(5), 861–872 (2007).

• Initial report that showed the establishment of human induced pluripotent stem cells.

7 Takahashi K, Yamanaka S. Induction of pluripotent stem cells from mouse embryonic and adult fibroblast cultures by defined factors. *Cell* 126(4), 663–676 (2006).

•• Initial report that showed the establishment of induced pluripotent stem cells.

8 Yu J, Vodyanik MA, Smuga-Otto K *et al.* Induced pluripotent stem cell lines derived from human somatic cells. *Science* 318(5858), 1917–1920 (2007).

• Initial report that showed the establishment of human induced pluripotent stem cells.

9 Park I-H, Zhao R, West JA *et al.* Reprogramming of human somatic cells to pluripotency with defined factors. *Nature* 451(7175), 141–146 (2008).

10 Okita K, Ichisaka T, Yamanaka S. Generation of germline-competent induced pluripotent stem cells. *Nature* 448(7151), 313–317 (2007).

11 Nak,agawa M, Koyanagi M, Tanabe K *et al.* Generation of induced pluripotent stem cells without Myc from mouse and human fibroblasts. *Nat. Biotech.* 26(1), 101–106 (2008).

12 Lowry WE, Richter L, Yachechko R *et al.* Generation of human induced pluripotent stem cells from dermal fibroblasts. *Proc. Natl Acad. Sci.* 105(8), 2883–2888 (2008).

13 Maherali N, Sridharan R, Xie W *et al.* Directly reprogrammed fibroblasts show global epigenetic remodeling and widespread tissue contribution. *Cell Stem Cell* 1(1), 55–70 (2007).

14 Hanna J, Markoulaki S, Schorderet P *et al.* Direct reprogramming of terminally differentiated mature B lymphocytes to pluripotency. *Cell* 133(2), 250–264 (2008).

15 Schenke-Layland K, Rhodes KE, Angelis E *et al.* Reprogrammed mouse fibroblasts differentiate into cells of the cardiovascular and hematopoietic lineages. *Stem Cells* 2008–0033 (2008).

16 Hanna J, Wernig M, Markoulaki S *et al.* Treatment of sickle cell anemia mouse model with IPS cells generated from autologous skin. *Science* 318(5858), 1920–1923 (2007).

17 Thomson JA, Itskovitz-Eldor J, Shapiro SS *et al.* Embryonic stem cell lines derived from human blastocysts. *Science* 282(5391), 1145–1147 (1998).

• Initial report that showed the establishment of human embryonic stem cells.

18 Wakayama T, Hayashi Y, Ogura A. Participation of the female pronucleus derived from the second polar body in full embryonic development of mice. *J. Reprod. Fertil.* 110(2), 263–266 (1997).

19 Doetschman TC, Eistetter H, Katz M, Schmidt W, Kemler R. The *in vitro* development of blastocyst-derived embryonic stem cell lines: formation of visceral yolk sac, blood islands and myocardium. *J. Embryol. Exp. Morphol.* 87, 27–45 (1985).

20 Klug MG, Soonpaa MH, Koh GY, Field LJ. Genetically selected cardiomyocytes from differentiating embronic stem cells form stable intracardiac grafts. *J. Clin. Invest.* 98(1), 216–224 (1996).

21 Hattan N, Kawaguchi H, Ando K *et al.* Purified cardiomyocytes from bone marrow mesenchymal stem cells produce stable intracardiac grafts in mice. *Cardiovasc. Res.* 65(2), 334–344 (2005).

22 Dyson E, Sucov HM, Kubalak SW *et al.* Atrial-Like Phenotype is Associated with Embryonic Ventricular Failure in Retinoid X Receptor {α} -/- Mice. *Proc. Natl Acad. Sci.* 92(16), 7386–7390 (1995).

23 Kastner P, Grondona JM, Mark M *et al.* Genetic analysis of RXRα developmental function: Convergence of RXR and RAR signaling pathways in heart and eye morphogenesis. *Cell* 78(6), 987–1003 (1994).

24 Osmond MK, Butler AJ, Voon FC, Bellairs R. The effects of retinoic acid on heart formation in the early chick embryo. *Development* 113(4), 1405–1417 (1991).

25 Edwards MK, Harris JF, McBurney MW. Induced muscle differentiation in an embryonal carcinoma cell line. *Mol. Cell. Biol.* 3(12), 2280–2286 (1983).

26 Wobus AM, Kaomei G, Shan J *et al.* Retinoic acid accelerates embryonic stem cell-derived cardiac differentiation and enhances development of ventricular cardiomyocytes. *J. Mol. Cell. Cardiol.* 29(6), 1525–1539 (1997).

27 Kanno S, Kim PKM, Sallam K, Lei J, Billiar TR, Shears LL 2nd. Nitric oxide facilitates cardiomyogenesis in mouse embryonic stem cells. *Proc. Natl Acad. Sci.* 101(33), 12277–12281 (2004).

28 Takahashi T, Lord B, Schulze PC *et al.* Ascorbic acid enhances differentiation of embryonic stem cells into cardiac myocytes. *Circulation* 107(14), 1912–1916 (2003).

29 Boheler KR, Czyz J, Tweedie D, Yang H-T, Anisimov SV, Wobus AM. Differentiation of pluripotent embryonic stem cells into cardiomyocytes. *Circ. Res.* 91(3), 189–201 (2002).

30 Sachinidis A, Fleischmann BK, Kolossov E, Wartenberg M, Sauer H, Hescheler J. Cardiac specific differentiation of mouse embryonic stem cells. *Cardiovasc. Res.* 58(2), 278–291 (2003).

31 Heng BC, Haider HK, Sim EK-W, Cao T, Ng SC. Strategies for directing the differentiation of stem cells into the cardiomyogenic lineage *in vitro*. *Cardiovasc. Res.* 62(1), 34–42 (2004).

32 Winnier G, Blessing M, Labosky PA, Hogan BL. Bone morphogenetic protein-4 is required for mesoderm formation and patterning in the mouse. *Genes Dev.* 9(17), 2105–2116 (1995).

33 Zhang H, Bradley A. Mice deficient for BMP2 are nonviable and have defects in amnion/chorion and cardiac development. *Development* 122(10), 2977–2986 (1996).

34 Schlange T, Andree B, Arnold H-H, Brand T. BMP2 is required for early heart development during a distinct time period. *Mech. Dev.* 91(1–2), 259–270 (2000).

35 Gaussin V, Van de Putte T, Mishina Y *et al.* Endocardial cushion and myocardial defects after cardiac myocyte-specific conditional deletion of the bone morphogenetic protein receptor ALK3. *Proc. Natl Acad. Sci.* 99(5), 2878–2883 (2002).

36 Marvin MJ, Di Rocco G, Gardiner A, Bush SM, Lassar AB. Inhibition of Wnt activity induces heart formation from posterior mesoderm. *Genes Dev.* 15(3), 316–327 (2001).

37 Schneider VA, Mercola M. Wnt antagonism initiates cardiogenesis in *Xenopus laevis*. *Genes Dev.* 15(3), 304–315 (2001).

38 Foley AC, Mercola M. Heart induction by Wnt antagonists depends on the homeodomain transcription factor Hex. *Genes Dev.* 19(3), 387–396 (2005).

39 Timmerman LA, Grego-Bessa J, Raya A *et al.* Notch promotes epithelial-mesenchymal transition during cardiac development and oncogenic transformation. *Genes Dev.* 18(1), 99–115 (2004).

127

40   Maillard I, Fang T, Pear WS. Regulation of lymphoid development, differentiation, and function by the notch pathway. *Ann. Rev. Immunol.* 23(1), 945–974 (2005).

41   Mima T, Ueno H, Fischman DA, Williams LT, Mikawa T. Fibroblast growth factor receptor is required for *in vivo* cardiac myocyte proliferation at early embryonic stages of heart development. *Proc. Natl Acad. Sci.* 92(2), 467–471 (1995).

42   von Bubnoff A, Cho KWY. Intracellular BMP signaling regulation in vertebrates: pathway or network? *Dev. Biol.* 239(1), 1–14 (2001).

43   Schneider MD, Gaussin V, Lyons KM. Tempting fate: BMP signals for cardiac morphogenesis. *Cytokine Growth Factor Rev.* 14(1), 1–4 (2003).

44   Hogan BLM. Bone morphogenetic proteins in development. *Curr. Opin. Gene. Dev.* 6(4), 432–438 (1996).

45   Ray RP, Wharton KA. Twisted perspective: new insights into extracellular modulation of bmp signaling during development. *Cell* 104(6), 801–804 (2001).

46   Lyons KM, Pelton RW, Hogan BL. Organogenesis and pattern formation in the mouse: RNA distribution patterns suggest a role for bone morphogenetic protein-2A (BMP-2A). *Development* 109(4), 833–844 (1990).

47   Lyons KM, Hogan BLM, Robertson EJ. Colocalization of BMP 7 and BMP 2 RNAs suggests that these factors cooperatively mediate tissue interactions during murine development. *Mech. Dev.* 50(1), 71–83 (1995).

48   Andrew T. Dudley EJR. Overlapping expression domains of bone morphogenetic protein family members potentially account for limited tissue defects in *BMP7* deficient embryos. *Dev. Dyn.* 208(3), 349–362 (1997).

49   Neuhaus H, Rosen V, Thies RS. Heart specific expression of mouse BMP-10 a novel member of the TGF-β superfamily. *Mech. Dev.* 80(2), 181–184 (1999).

50   Schultheiss TM, Burch JB, Lassar AB. A role for bone morphogenetic proteins in the induction of cardiac myogenesis. *Genes Dev.* 11(4), 451–462 (1997).

51   Monzen K, Hiroi Y, Kudoh S *et al.* Smads, TAK1, and their common target atf-2 play a critical role in cardiomyocyte differentiation. *J. Cell Biol.* 153(4), 687–698 (2001).

52   Monzen K, Shiojima I, Hiroi Y *et al.* Bone morphogenetic proteins induce cardiomyocyte differentiation through the mitogen-activated protein kinase kinase kinase TAK1 and cardiac transcription factors Csx/Nkx-2.5 and GATA-4. *Mol. Cell. Biol.* 19(10), 7096–7105 (1999).

53   Ladd AN, Yatskievych TA, Antin PB. Regulation of avian cardiac myogenesis by activin/TGFβ and bone morphogenetic proteins. *Dev. Biol.* 204(2), 407–419 (1998).

54   Sasai Y, Lu B, Steinbeisser H, De Robertis EM. Regulation of neural induction by the Chd and Bmp-4 antagonistic patterning signals in *Xenopus. Nature* 376(6538), 333–336 (1995).

55   Lim DA, Tramontin AD, Trevejo JM, Herrera DG, Garcia-Verdugo JM, Alvarez-Buylla A. Noggin antagonizes BMP signaling to create a niche for adult neurogenesis. *Neuron* 28(3), 713–726 (2000).

56   Faure S, de Santa Barbara P, Roberts DJ, Whitman M. Endogenous patterns of BMP signaling during early chick development. *Dev. Biol.* 244(1), 44–65 (2002).

57   Fletcher RB, Watson AL, Harland RM. Expression of *Xenopus tropicalis* noggin1 and noggin2 in early development: two noggin genes in a tetrapod. *Gene Expr. Patterns* 5(2), 225–230 (2004).

58   Zhang P, Li J, Tan Z *et al.* Short-term BMP-4 treatment initiates mesoderm induction in human embryonic stem cells. *Blood* 111(4), 1933–1941 (2008).

59   Kumar D, Sun B. Transforming growth factor-β2 enhances differentiation of cardiac myocytes from embryonic stem cells. *Biochem. Biophys. Res. Commun.* 332(1), 135–141 (2005).

60   Behfar A, Zingman LV, Hodgson DM *et al.* Stem cell differentiation requires a paracrine pathway in the heart. *FASEB J.* 16(12), 1558–1566 (2002).

61   Laflamme MA, Chen KY, Naumova AV *et al.* Cardiomyocytes derived from human embryonic stem cells in pro-survival factors enhance function of infarcted rat hearts. *Nat. Biotech.* 25(9), 1015–1024 (2007).

62   Reya T, Clevers H. Wnt signalling in stem cells and cancer. *Nature* 434(7035), 843–850 (2005).

63   Charron F, Tessier-Lavigne M. Novel brain wiring functions for classical morphogens: a role as graded positional cues in axon guidance. *Development* 132(10), 2251–2262 (2005).

64   Bejsovec A. Wnt pathway activation: new relations and locations. *Cell* 120(1), 11–14 (2005).

65   Widelitz R. Wnt signaling through canonical and non-canonical pathways: recent progress. *Growth Factors* 23(2), 111–116 (2005).

66   Chapman SC, Brown R, Lees L, Schoenwolf GC, Lumsden A. Expression analysis of chick Wnt and frizzled genes and selected inhibitors in early chick patterning. *Dev. Dyn.* 229(3), 668–676 (2004).

67   Eisenberg CA, Gourdie RG, Eisenberg LM. Wnt-11 is expressed in early avian mesoderm and required for the differentiation of the quail mesoderm cell line QCE-6. *Development* 124(2), 525–536 (1997).

68   Carol A. Eisenberg LME. WNT11 promotes cardiac tissue formation of early mesoderm. *Dev. Dyn.* 216(1), 45–58 (1999).

69   Pandur P, Lasche M, Eisenberg LM, Kuhl M. Wnt-11 activation of a non-canonical Wnt signalling pathway is required for cardiogenesis. *Nature* 418(6898), 636–641 (2002).

70   Terami H, Hidaka K, Katsumata T, Iio A, Morisaki T. Wnt11 facilitates embryonic stem cell differentiation to Nkx2.5-positive cardiomyocytes. *Biochem. Biophys. Res. Commun.* 325(3), 968–975 (2004).

71   Nakamura T, Sano M, Songyang Z, Schneider MD. A Wnt- and β -catenin-dependent pathway for mammalian cardiac myogenesis. *Proc. Natl Acad. Sci.* 100(10), 5834–5839 (2003).

72   Deb A, Davis BH, Guo J *et al.* SFRP2 regulates cardiomyogenic differentiation by inhibiting a positive transcriptional autofeedback loop of Wnt3a. *Stem Cells* 26(1), 35–44 (2008).

73   Kwon C, Arnold J, Hsiao EC, Taketo MM, Conklin BR, Srivastava D. Canonical Wnt signaling is a positive regulator of mammalian cardiac progenitors. *Proc. Natl Acad. Sci.* 104(26), 10894–10899 (2007).

74   Ai D, Fu X, Wang J *et al.* Canonical Wnt signaling functions in second heart field to promote right ventricular growth. *Proc. Natl Acad. Sci.* 104(22), 9319–9324 (2007).

75   Liu Y, Asakura M, Inoue H *et al.* Sox17 is essential for the specification of cardiac mesoderm in embryonic stem cells. *Proc. Natl Acad. Sci.* 104(10), 3859–3864 (2007).

76 Naito AT, Shiojima I, Akazawa H *et al.* Developmental stage-specific biphasic roles of Wnt/β-catenin signaling in cardiomyogenesis and hematopoiesis. *Proc. Natl Acad. Sci.* 103(52), 19812–19817 (2006).

77 Ueno S, Weidinger G, Osugi T *et al.* From the cover: biphasic role for Wnt/β-catenin signaling in cardiac specification in zebrafish and embryonic stem cells. *Proc. Natl Acad. Sci.* 104(23), 9685–9690 (2007).

78 Singh AM, Li F-Q, Hamazaki T, Kasahara H, Takemaru K-I, Terada N. Chibby, an antagonist of the Wnt/β-catenin pathway, facilitates cardiomyocyte differentiation of murine embryonic stem cells. *Circulation* 115(5), 617–626 (2007).

79 Artavanis-Tsakonas S, Rand MD, Lake RJ. Notch signaling: cell fate control and signal integration in development. *Science* 284(5415), 770–776 (1999).

80 Lutolf S, Radtke F, Aguet M, Suter U, Taylor V. Notch1 is required for neuronal and glial differentiation in the cerebellum. *Development* 129(2), 373–385 (2002).

81 Yoon K, Gaiano N. Notch signaling in the mammalian central nervous system: insights from mouse mutants. *Nat. Neurosci.* 8(6), 709–715 (2005).

82 Radtke F, Raj K. The role of Notch in tumorigenesis: oncogene or tumour suppressor? *Nat. Rev. Cancer* 3(10), 756–767 (2003).

83 Schroeder T, Fraser ST, Ogawa M *et al.* Recombination signal sequence-binding protein Jκ alters mesodermal cell fate decisions by suppressing cardiomyogenesis. *Proc. Natl Acad. Sci.* 100(7), 4018–4023 (2003).

84 Nemir M, Croquelois A, Pedrazzini T, Radtke F. Induction of cardiogenesis in embryonic stem cells via downregulation of Notch1 signaling. *Circ. Res.* 98(12), 1471–1478 (2006).

85 Garg V, Muth AN, Ransom JF *et al.* Mutations in NOTCH1 cause aortic valve disease. *Nature* 437(7056), 270–274 (2005).

86 Grego-Bessa J, Luna-Zurita L, del Monte G *et al.* Notch signaling is essential for ventricular chamber development. *Developmental Cell* 12(3), 415–429 (2007).

87 Kwon C, Han Z, Olson EN, Srivastava D. MicroRNA1 influences cardiac differentiation in Drosophila and regulates Notch signaling. *Proc. Natl Acad. Sci.* 102(52), 18986–18991 (2005).

88 Bussell K. The dynamics of the cycle. *Nat. Rev. Mol. Cell. Biol.* 6(3), 190–190 (2005).

89 Lum L, Beachy PA. The hedgehog response network: sensors, switches, and routers. *Science* 304(5678), 1755–1759 (2004).

90 Kehat I, Kenyagin-Karsenti D, Snir M *et al.* Human embryonic stem cells can differentiate into myocytes with structural and functional properties of cardiomyocytes. *J. Clin. Invest.* 108(3), 407–414 (2001).

91 Kehat I, Khimovich L, Caspi O *et al.* Electromechanical integration of cardiomyocytes derived from human embryonic stem cells. *Nat. Biotechnol.* 22(10), 1282–1289 (2004).

92 Schachinger V, Erbs S, Elsasser A *et al.* Intracoronary bone marrow-derived progenitor cells in acute myocardial infarction. *N. Engl. J. Med.* 355(12), 1210–1221 (2006).

93 Janssens S, Dubois C, Bogaert J *et al.* Autologous bone marrow-derived stem-cell transfer in patients with ST-segment elevation myocardial infarction: double-blind, randomised controlled trial. *Lancet* 367(9505), 113–121 (2006).

94 Lunde K, Solheim S, Aakhus S *et al.* Intracoronary Injection of mononuclear bone marrow cells in acute myocardial infarction. *N. Engl. J. Med.* 355(12), 1199–1209 (2006).

Affiliations

- Shinsuke Yuasa, MD, PhD
  Assistant Professor, Cardiology Division, Department of Medicine; and, Department of Regenerative Medicine and Advanced Cardiac Therapeutics, Keio University School of Medicine, 35-Shinanomachi Shinjuku-ku Tokyo, 160-8582, Japan
  Tel.: +81 333 531 211 ext. 62310
  Fax: +81 333 532 502
  shinsuke@cpnet.med.keio.ac.jp

- Keiichi Fukuda, MD, PhD, FACC
  Professor and Chair, Department of Regenerative Medicine and Advanced Cardiac Therapeutics, Keio University School of Medicine, 35 Shinanomachi, Shinjuku, Tokyo 160-8582, Japan
  Tel.: +81 353 633 874
  Fax: +81 353 633 875
  kfukuda@sc.itc.keio.ac.jp

Ontogeny and Multipotency of Neural Crest-Derived Stem Cells in Mouse Bone Marrow, Dorsal Root Ganglia, and Whisker Pad

Narihito Nagoshi,[1,2] Shinsuke Shibata,[1] Yoshiaki Kubota,[3] Masaya Nakamura,[2] Yasuo Nagai,[1] Etsuko Satoh,[1] Satoru Morikawa,[1,4] Yohei Okada,[1,6] Yo Mabuchi,[1] Hiroyuki Katoh,[2] Seiji Okada,[1,7] Keiichi Fukuda,[5] Toshio Suda,[3] Yumi Matsuzaki,[1] Yoshiaki Toyama,[2] and Hideyuki Okano[1,*]

[1]Department of Physiology
[2]Department of Orthopedic Surgery
[3]Department of Cell Differentiation
[4]Department of Dentistry and Oral Surgery
[5]Department of Regenerative Medicine and Advanced Cardiac Therapeutics
Keio University School of Medicine, 35 Shinanomachi, Shinjuku-ku, Tokyo 160-8582, Japan
[6]Department of Neurology, Nagoya University Graduate School of Medicine, 65 Tsurumai-cho, Showa-ku, Nagoya 466-8550, Japan
[7]SSP Stem Cell Unit, Graduate School of Medical Science, Kyushu University, 3-1-1 Maidashi, Higashi-ku, Fukuoka 812-8582, Japan
*Correspondence: hidokano@sc.itc.keio.ac.jp
DOI 10.1016/j.stem.2008.03.005

SUMMARY

Although recent reports have described multipotent, self-renewing, neural crest-derived stem cells (NCSCs), the NCSCs in various adult rodent tissues have not been well characterized or compared. Here we identified NCSCs in the bone marrow (BM), dorsal root ganglia, and whisker pad and prospectively isolated them from adult transgenic mice encoding neural crest-specific P0-Cre/Floxed-EGFP and Wnt1-Cre/Floxed-EGFP. Cultured EGFP-positive cells formed neurosphere-like structures that expressed NCSC genes and could differentiate into neurons, glial cells, and myofibroblasts, but the frequency of the cell types was tissue source dependent. Interestingly, we observed NCSCs in the aorta-gonad-mesonephros region, circulating blood, and liver at the embryonic stage, suggesting that NCSCs migrate through the bloodstream to the BM and providing an explanation for how neural cells are generated from the BM. The identification of NCSCs in accessible adult tissue provides a new potential source for autologous cell therapy after nerve injury or disease.

INTRODUCTION

The neural crest is a transient embryonic tissue that originates at the neural folds during vertebrate development. Neural crest cells delaminate from the dorsal neural tube and migrate to various locations, where they differentiate into a vast range of cells, including neurons and glial cells of the autonomic and enteric nervous systems, smooth muscle cells of the heart and great vessels, and bone and cartilage cells of the face (Le Douarin and Kalcheim, 1999).

From the embryonic period through adulthood, neural crest cells are generated by neural crest-derived stem cells (NCSCs), which

are self-renewing and multipotent, with the potential to differentiate into neurons, glial cells, and myofibroblasts (Morrison et al., 1999; Shah et al., 1996). NCSCs have been isolated from the embryonic sciatic nerve (Morrison et al., 1999) and boundary cap (BC) (Hjerling-Leffler et al., 2005) and the gut (Kruger et al., 2002), skin (Fernandes et al., 2004; Sieber-Blum et al., 2004; Wong et al., 2006), heart (Tomita et al., 2005), and cornea (Yoshida et al., 2006) of adult rodents. These reports demonstrate the presence of NCSCs in these tissues and suggest their existence in other adult tissues.

Several types of stem cells have been identified in adult tissues. For example, several groups have described multipotent stem cells in the bone marrow (BM), but the developmental origin and differentiation potential of these cells are unknown (D'Ippolito et al., 2004; Jiang et al., 2002; Ross et al., 2006). These stem cells are reported to generate neural cells and smooth muscle cells, which are known to originate from neural crest cells. Such observations led us to investigate whether some newly identified stem cells might be NCSCs. We examined this hypothesis by investigating various tissues of double-transgenic mice encoding Protein-0 (P0) and Wnt1 promoter-Cre/Floxed-EGFP, in which neural crest-derived cells express EGFP (Danielian et al., 1998; Kawamoto et al., 2000; Yamauchi et al., 1999).

Here, we prospectively isolated and compared neural crest-derived stem and progenitor cells from the BM of the lower extremities, dorsal root ganglia (DRG), and whisker pad (WP) of adult P0 and Wnt1 promoter-Cre/Floxed-EGFP mice. This is the first report identifying NCSCs in the BM of adult rodents. The existence of NCSCs was confirmed in all three tissues, and distinct differences among the NCSCs were revealed by comparing their proliferation capacity, differentiation potential, and gene expression profiles.

RESULTS

Distribution of EGFP-Positive Neural Crest-Lineage Cells in Embryonic and Adult P0 and Wnt1-Cre/Floxed-EGFP Mice

To examine the distribution of neural crest-derived cells in various tissues, we performed histological analyses of
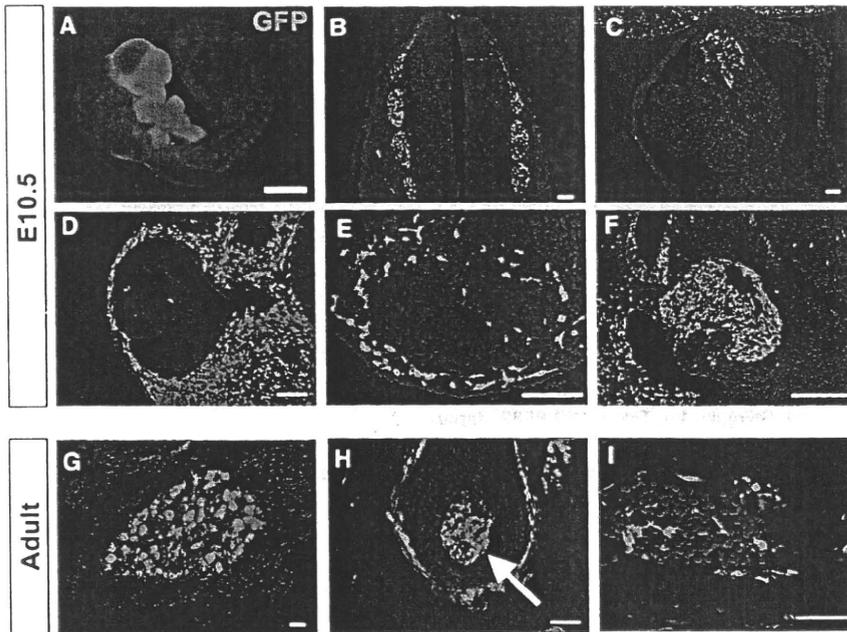
Figure 1. Expression Pattern of EGFP in P0-Cre/Floxed-EGFP Mice at E10.5 and the Adult Stage

(A) Whole-body observation of direct EGFP fluorescence in E10.5 mice.

(B–F) Anti-GFP immunostaining of E10.5 mice revealed EGFP+ cells in the DRG (B), outflow tract of the heart (C), optic mesenchyme (D), gut (E), and trigeminal ganglion (F).

(G–I) In 8-week-old adult mice, EGFP+ cells were detected in the DRG (G), dermal papilla in the whisker follicle (arrow in [H]), and BM of the tibia (I). Scale bars, 1 mm in (A) and 50 μm in (B)–(I).

P0-Cre/Floxed-EGFP mouse embryos and adults. P0 was originally identified as a Schwann cell-specific myelin protein (Lemke et al., 1988), but it is also expressed by migrating neural crest cells during the early embryonic period in chicks (Bhattacharyya et al., 1991). In this transgenic mouse, the transient activation of the P0 promoter induces Cre-mediated recombination, indelibly tagging neural crest-derived cells with EGFP expression (Kawamoto et al., 2000; Yamauchi et al., 1999). At E10.5, EGFP was observed in the pharyngeal arches, periocular region, and front nasal region, which contain neural crest-derived cells (Figure 1A) (Yamauchi et al., 1999). Anti-GFP immunostaining of E10.5 embryos revealed EGFP-positive (EGFP+) cells in the DRG, outflow tract of the aorta, optic mesenchyme, gut, and trigeminal ganglia (Figures 1B–1F). In adult mice, EGFP+ cells were observed in the DRG, dermal papilla of whisker follicles, and BM of the tibia (Figures 1G–1I). As a negative control, we examined anti-GFP staining in single transgenic P0-Cre mice without the Floxed-EGFP reporter and detected no EGFP+ cells (data not shown), confirming the validity of the anti-GFP staining. Immunohistochemistry was also performed on various tissues from adult Wnt1-Cre/Floxed-EGFP mice, confirming the presence of EGFP+ cells in the DRG, dermal papilla, and BM (see Figure S1 available online). These observations suggest that EGFP+ neural crest-derived cells migrate to and survive in various adult tissues.

Since neural crest-derived cells have not been previously reported in the BM, we analyzed the distribution of EGFP+ cells in the BM of P0-Cre/Floxed-EGFP mice by immunohistochemistry. It is unlikely that EGFP expression was induced by the ectopic expression of P0, since we did not detect P0 protein in the BM (Figure S2). In the BM of P0-Cre/Floxed-EGFP mice, EGFP+ cells were detected along blood vessels, especially the vasculature located near the inner surface of the bone cortex (Figures 2A–2C). In whole-mount specimens, these EGFP+ cells were positive for both PECAM-1 and SMA, markers for endothelial cells and smooth muscle cells (Figures 2E–2L), and quantitative analysis revealed that 3.85% and 6.23% of the EGFP+ cells

in the BM were positive for PECAM-1 and SMA, respectively. The contribution of EGFP+ cells to the vascular endothelial structure was also confirmed by flow-cytometric analysis (Figure 2D) and whole-mount immunohistochemistry with other vascular markers (Figures 2M–2X). Although a portion of vascular smooth muscle cells are known to be derived from the neural crest, neural crest-derived cells have not been reported in the vascular endothelium in previous studies (Etchevers et al., 2001; Joseph et al., 2004). To corroborate our observations, we examined the BM in adult Wnt1-Cre/Floxed-EGFP mice. Although a similar number of EGFP+ cells was observed, the EGFP+ cells did not express endothelial cell or smooth muscle cell markers (Figures S1C and S1D). Thus, our detailed analyses using two lines of transgenic mice demonstrated the presence of neural crest-derived cells in the BM, but their contribution to blood vessel formation remains unclear.

NCSCs Migrate from the Trunk Dorsal Neural Tube to the Aorta-Gonad-Mesonephros Region and Circulate in the Blood during Embryonic Development

To elucidate the migration route of EGFP+ cells from the trunk dorsal neural tube to the BM, we focused on the aorta-gonad-mesonephros (AGM) region in P0 and Wnt1-Cre/Floxed-EGFP mice. During development, the first adult-type hematopoietic stem cells (HSCs) are generated at E10.5 in the AGM region and migrate via the blood stream to the BM in the late embryonic period (Medvinsky and Dzierzak, 1996; Muller et al., 1994). Mesenchymal stem cells (MSCs) are also generated in the AGM region at E11.0, migrate in the blood stream, and are found in the neonatal BM (Mendes et al., 2005). We therefore hypothesized that neural crest-derived cells take a similar route to the BM, migrating from the dorsal neural tube to the AGM region, from which they then travel through the blood stream to the BM. Anti-GFP immunostaining revealed EGFP+ cells migrating from the trunk dorsal neural tube to the AGM region in E11.0 P0-Cre/Floxed-EGFP mice (Figure 3A). These EGFP+ cells were 100% positive for p75 and 50.6% positive for Sox10, both known as NCSC markers (Paratore et al., 2001; Stemple and Anderson, 1992) (Figures 3B and 3C), suggesting that a portion of the EGFP+ cells in the AGM region were NCSCs. At E12.5, most of the EGFP+ cells were positive for tyrosine hydroxylase
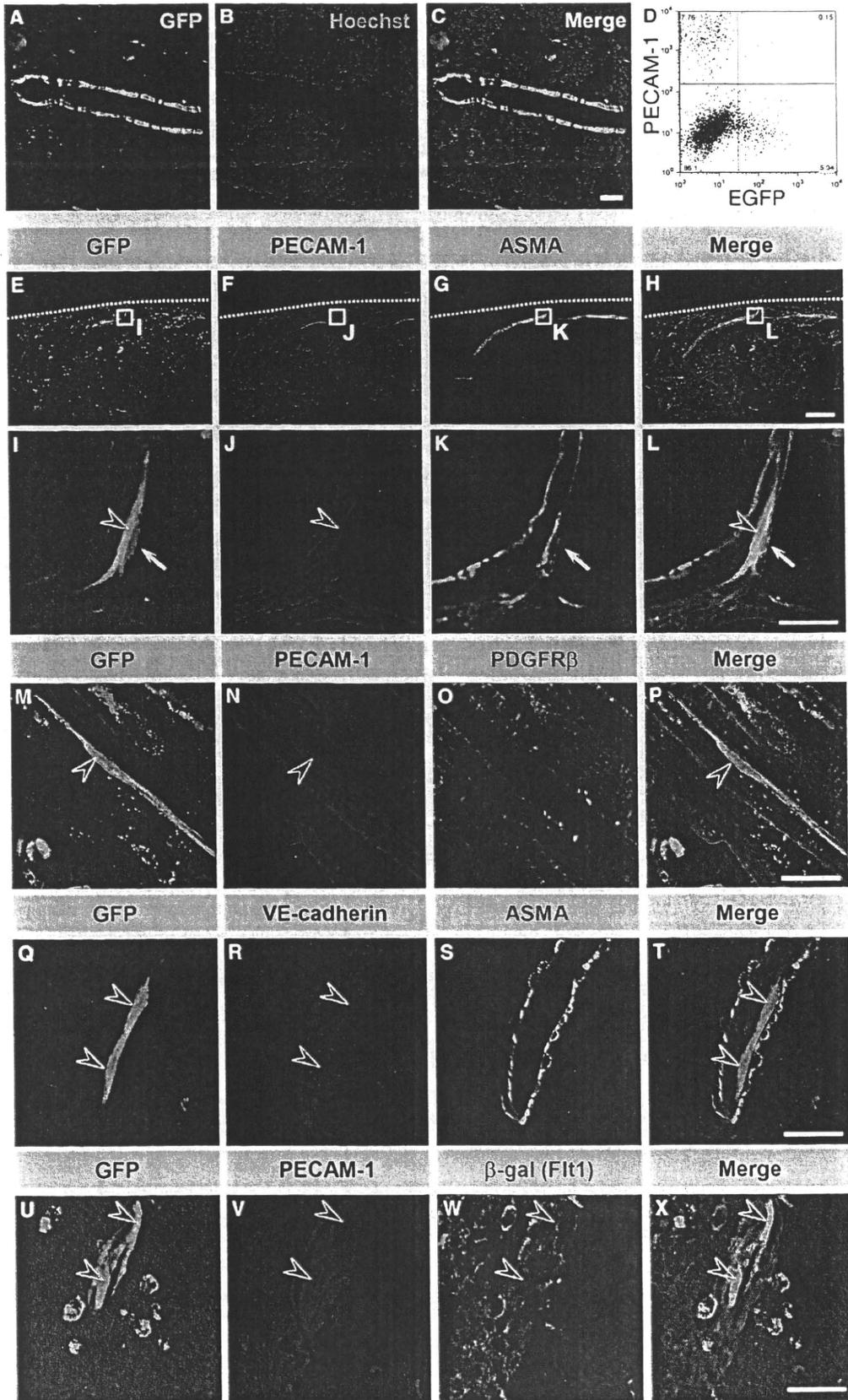
(TH), a marker of catecholaminergic neurons that make up the para-aortic plexus (Figure 3D), raising the possibility that EGFP$^+$ Sox10$^-$ cells at E11.0 were neuroblasts that differentiated into TH$^+$ neurons at E12.5. However, the small number of TH$^-$ EGFP$^+$ cells that invaded the aorta were positive for p75 and Sox10 (Figures 3E–3H), suggesting that the cells entering the blood vessel were NCSCs. None of the EGFP$^+$ cells at the periphery of aorta were positive for GFAP (Figure 3I), ruling out the possibility that the EGFP$^+$ cells are newly arrived Schwann cells that are migrating along the vasculature. EGFP$^+$ p75$^+$ cells were also observed in peripheral blood at E12.5 by immunohistochemistry (Figures 3J and 3K), and flow-cytometric analysis of the blood taken from E13.5 to E15.5 mice detected EGFP$^+$ cells (Figure 3L). In E14.5 mice, immunohistochemistry revealed EGFP$^+$ Sox10$^+$ cells in the fetal liver (Figures 3M and 3N). After E18.5, no EGFP$^+$ cells were detected in the circulating blood (Figure 3L). Similar results were observed in the AGM region, peripheral blood, and fetal liver in Wnt1-Cre/Floxed-EGFP mice (Figure S3). These observations suggest that NCSCs migrate in the blood to the BM via the AGM region, specifically during E12.5–E15.5, similar to HSCs.

Sphere-Forming Capability of Neural Crest-Derived Cells from Adult Mice

To compare neural crest-derived cells from the DRG, WP, and BM, cells from these tissues were collected from postnatal 2-, 4-, 8-, and 13-week-old P0-Cre/Floxed-EGFP mice, and their EGFP expression was analyzed by flow cytometry. The frequency of EGFP$^+$ cells from each source was highest at 2 weeks of age and decreased over time (Figures 4A and 4B). The same result was observed in Wnt1-Cre/Floxed-EGFP mice (Figure S4A). Interestingly, the number of EGFP$^+$ cells collected from the BM increased when the bones were treated with collagenase. Since collagenase releases BM cells that adhere tightly to the bone (Funk et al., 1994), this suggests that the neural crest-derived cells observed histologically were tightly associated with the BM surface.

The formation of neurosphere-like spheres from neural crest-derived tissue has been reported (Fernandes et al., 2004; Tomita et al., 2005; Yoshida et al., 2006) using culture procedures similar to neurosphere-culture protocols for cells of the central nervous system (CNS) (Reynolds and Weiss, 1992). To confirm the capability of neural crest-derived cells to proliferate and form spheres, EGFP$^+$ and EGFP$^-$ cells from the DRG, WP, and BM of 8-week-old P0-Cre/Floxed-EGFP mice were collected by flow cytometry and cultured at a density of 5 × 10^3 cells/ml (Hulspas et al., 1997) in serum-free sphere-forming

medium containing human epidermal growth factor (EGF), human fibroblast growth factor 2 (FGF2), and B27. The EGFP$^+$ cells proliferated to form spheres that were morphologically similar to CNS neurospheres after 14 days (Figure 4C). When cultured at the same density, the highest number of spheres was formed from cells derived from the DRG and the lowest from the BM (Figure 4D). Cultured EGFP$^-$ cells derived from the DRG and BM did not form spheres, but those from the WP did, albeit at a much lower frequency than the EGFP$^+$ cells (Figure 4D). Sphere-forming capacity and tissue-specific sphere-forming efficacy in cells from adult Wnt1-Cre/Floxed-EGFP mice were similar to those from P0-Cre/Floxed-EGFP mice (Figures S4B and S4C). These results indicate that neural crest-derived cells capable of proliferating into spheres exist in the adult DRG and BM in addition to the WP, which has been previously reported.

Spheres Derived from Each Adult Tissue Contain Multipotent NCSCs

Previous reports have characterized NCSCs by their ability to self-renew and their capacity for multilineage differentiation (multipotency) into neurons, glial cells, and myofibroblasts (Morrison et al., 1999; Shah et al., 1996). To evaluate the differentiation potential of EGFP$^+$ spheres generated from sorted EGFP$^+$ cells, we cultured EGFP$^+$ spheres from the three tissue sources of adult P0-Cre/Floxed-EGFP mice for 10 days in 10% serum-containing differentiation medium. The differentiated cells were identified by triple immunostaining: neurons by β-III tubulin, glial cells by glial fibrillary acidic protein (GFAP), and myofibroblasts by SMA. EGFP$^+$ spheres from all three sources demonstrated trilineage differentiation potential (Figure 5A), but the differentiation preference differed depending on the tissue source (Table 1). Most of the DRG-derived spheres showed trilineage differentiation potential (NGM, 74.6%), but the frequency was significantly lower in the WP- and BM-derived spheres (NGM, 7.3% and 3.3%, respectively). The WP-derived spheres displayed a bilineage differentiation tendency into neurons and myofibroblasts (NM, 91.6%), while most BM-derived spheres differentiated into myofibroblasts (M, 64.6%), suggesting that EGFP$^+$ cells derived from the WP and BM are mostly lineage-restricted progenitors, with only a small percentage possessing multilineage differentiation potential. In addition, when EGFP$^+$ DRG-derived spheres were cultured in differentiation medium containing 5-bromo-2'-deoxyuridine (BrdU) (Figure 5B), all three resulting cell types (N, M, and G) were positive for BrdU. Therefore, these three cell types from DRG-derived spheres probably originated from mitotic precursor cells within the

---

Figure 2. EGFP$^+$ Cells Contribute to Vascular Endothelial and Smooth Muscle Cells in the BM of P0-Cre/Floxed-EGFP Mice

(A–C) EGFP$^+$ cells were detected along vasculature in the tibia.

(D) Representative EGFP- and PECAM-1-gated flow-cytometric analysis chart. To prevent the contamination of macrophages, CD45$^+$ cells were removed before analysis.

(E–L) Triple immunohistochemistry for GFP, PECAM-1, and SMA in whole-mount specimens. Note the abundant EGFP$^+$ cells around the inner surface of the bone cortex (outer surface indicated by dotted lines). (I–L) High-magnification views of the boxed areas in (E)–(H), respectively. Note the EGFP$^+$ endothelial cells (arrowheads) and smooth muscle cells (arrows).

(M–P) Triple immunohistochemistry for GFP, PECAM-1, and PDGFRβ, a marker for pericytes and smooth muscle cells. The arrowhead indicates EGFP$^+$ PECAM-1$^+$ endothelial cells.

(Q–T) EGFP$^+$ cells were also positive for VE-cadherin, a marker for endothelial cells (arrowheads).

(U–X) In triple-transgenic mice encoding P0-Cre/Floxed-EGFP/Flt1^{lacZ}, EGFP$^+$ cells were positive for PECAM-1 and β-gal (arrowheads). Flt1 is expressed in endothelial and hematopoietic cells. Scale bars, 50 μm in (A)–(C), 200 μm in (E)–(H), and 20 μm in (I)–(X).
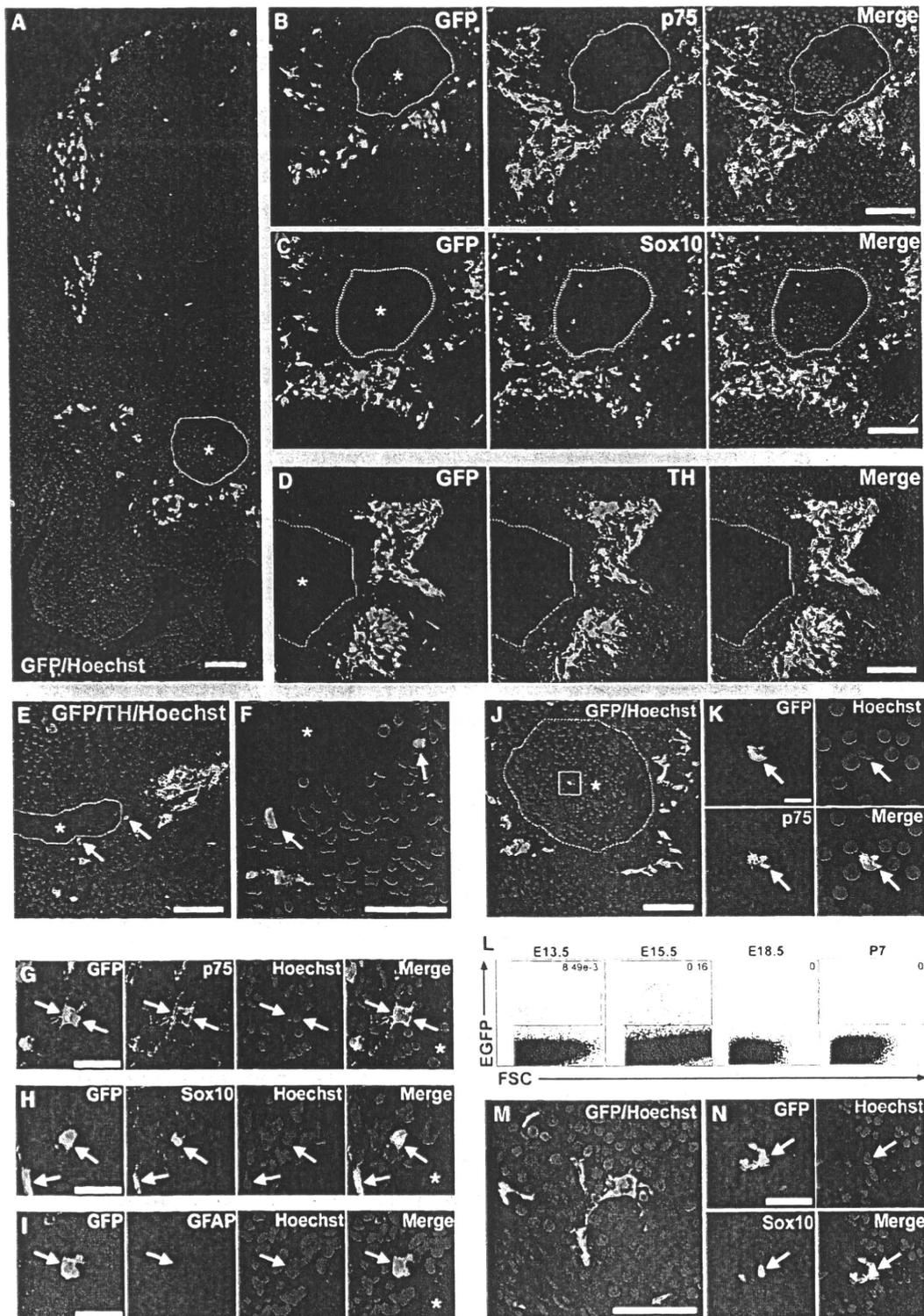
Figure 3. Histological Analyses of the AGM Region and Flow-Cytometric Analyses of Peripheral Blood in P0-Cre/Floxed-EGFP Mice

(A) At E11.0, EGFP+ cells detected by anti-GFP antibodies were seen migrating from the dorsal neural tube into the AGM region. The region enclosed in a dashed line with an asterisk indicates the aorta.

(B and C) Double immunohistochemistry of the AGM region revealed that EGFP+ cells were positive for p75 (B) and partially colocalized with Sox10 (C), indicating that EGFP+ cells in the embryonic AGM region expressed NCSC markers.

(D–F) At E12.5, most EGFP+ cells had differentiated into TH-positive catecholaminergic neurons (D), but some EGFP+ TH⁻ cells invaded the aorta (arrows in [E] and [F]).
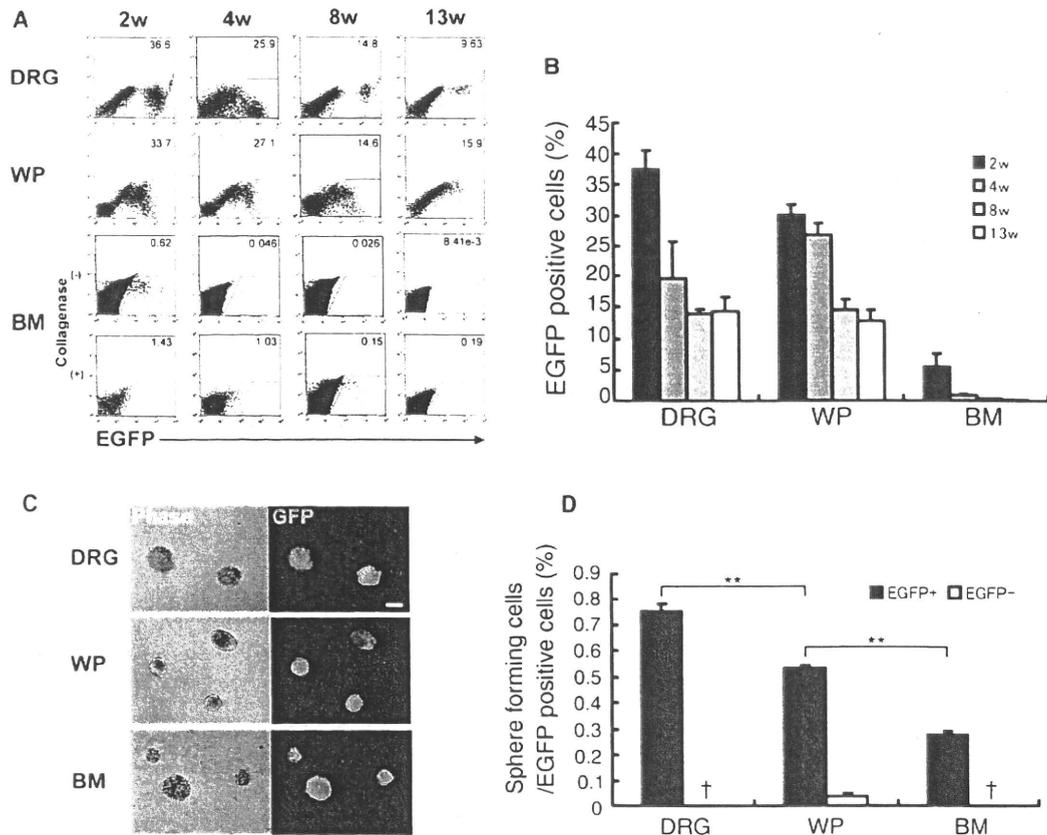
Figure 4. Isolation and Sphere-Forming Capacity of Neural Crest-Lineage Cells Derived from the DRG, WP, and BM in Adult P0-Cre/Floxed-EGFP Mice

(A) Representative EGFP-gated flow-cytometric analysis charts of cells from the DRG, WP, and BM of postnatal 2-, 4-, 8-, and 13-week-old mice. In the BM, the number of collected EGFP⁺ cells increased with collagenase treatment.

(B) The number of collected EGFP⁺ cells from all three sources decreased with age (mean ± SEM, n = 3 per group).

(C) Phase-contrast and direct EGFP-fluorescent images showing spheres formed from EGFP⁺ cells after 14 days in culture. Scale bar, 50 μm.

(D) The percentage of sphere-forming cells found in each tissue source was assessed by culturing EGFP⁺ and EGFP⁻ cells from each source at a cell density of 5×10^3 cells/ml and counting the number of spheres formed (mean ± SEM; n = 3 per group; **p < 0.01; †, no sphere observed). The highest percentage of sphere-forming cells was observed in the DRG, and the WP was the only source with EGFP⁻ cells capable of forming spheres.

spheres and did not represent contamination of postmitotic cells from the original tissue.

Recent reports have questioned the validity of "clonal density" cultures (Jessberger et al., 2007; Singec et al., 2006), demonstrating that CNS neurospheres are motile structures that can fuse even at cellular concentrations previously regarded as "clonal" (Hulspas et al., 1997). To assess the possible effects of sphere fusion in our culture protocol, we examined the differentiation of spheres cultured in medium containing 0.8% methylcellulose (Figures S5A–S5C). This method, which we previously reported (Yoshida et al., 2006), effectively prevents sphere fusion, resulting in spheres that are more than 90% clonal. Differentiation studies of these clonal spheres yielded results similar to those shown in Table 1 (Figure S5D), indicating

that the influence of sphere fusion was quite limited. Results from adult Wnt1-Cre/Floxed-EGFP mice corroborated data from adult P0-Cre/Floxed-EGFP mice, revealing the formation of clonal spheres from the DRG, WP, and BM that possessed a similar differentiation preference (Figures S4B–S4E).

To assess the self-renewal capacity of the EGFP⁺ spheres, secondary sphere-forming assays were conducted. EGFP⁺ spheres derived from each tissue source of P0-Cre/Floxed-EGFP mice were independently placed into one well of a 96-well plate, dissociated into single cells, and cultured in sphere-forming medium. The frequency of secondary sphere formation was highest in cells derived from the DRG (Figure 5C), confirming that, of these three sources, the DRG contains the highest frequency of NCSCs.

(G–I) At E12.5, most EGFP⁺ cells at the periphery of the aorta were positive for p75 and Sox10 but negative for GFAP.

(J and K) EGFP⁺ p75⁺ cells were observed in the peripheral blood of E12.5 mice (boxed area in [J] magnified in [K]).

(L) EGFP-gated flow-cytometric analysis charts of embryonic and postnatal blood cells. EGFP⁺ cells were detected from E13.5 and E15.5, but not at E18.5 or after birth. Transverse axis indicates forward scatter (FSC).

(M and N) At E14.5, EGFP⁺ cells were observed in the liver. Some were positive for Sox10, indicating that NCSCs exist in the liver. Scale bars, 100 μm in (A)–(F), (J), and (M); 50 μm in (G)–(I), and (N); and 20 μm in (K).
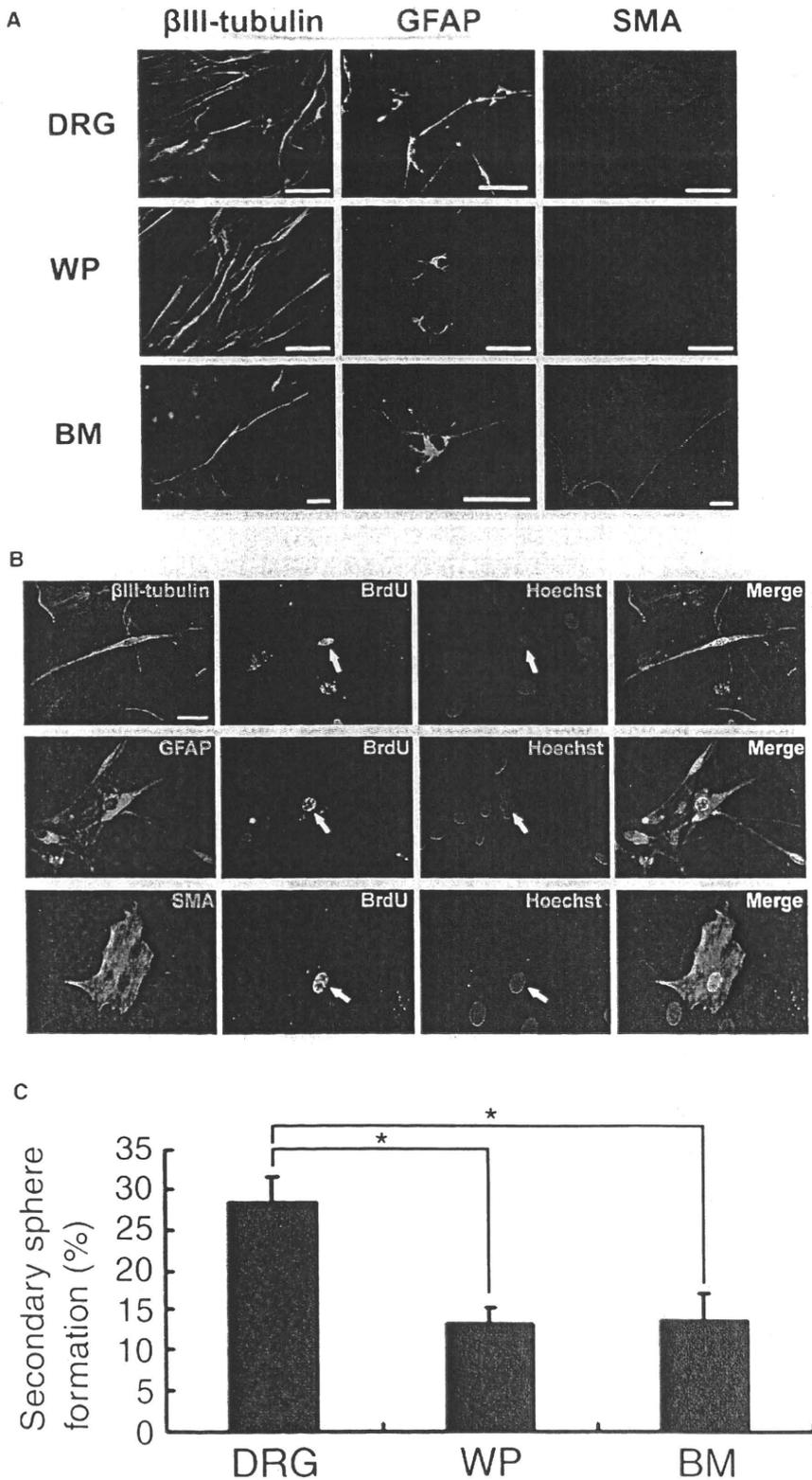
A

B

C

Figure 5. Differentiation and Secondary Sphere-Forming Capacity of EGFP⁺ Spheres Derived from the DRG, WP, and BM in Adult P0-Cre/Floxed-EGFP Mice

(A) EGFP⁺ spheres formed from each tissue source differentiated into neurons, glial cells, and myofibroblasts. Scale bars, 50 μm.

(B) DRG-derived spheres were cultured in medium containing BrdU. Cells double positive for BrdU and each cell-type-specific marker were observed. Scale bar, 25 μm.

(C) When these spheres were dissociated, the DRG-derived cells formed the greatest number of secondary spheres, indicating their high capacity for self-renewal (mean ± SEM; n = 3 per group; *p < 0.05).

EGFP mice were analyzed by semiquantitative RT-PCR for various markers, especially neural crest-associated genes (Figure 6A). The following were prepared from each adult tissue source: noncultured EGFP⁻ and EGFP⁺ cells, cultured spheres, and cells differentiated from spheres. The noncultured cells showed varying tissue-source-dependent gene expression patterns. EGFP⁺ cells from the DRG strongly expressed the known NCSC markers *Sox10* and *p75*. Although their expression of the neural crest markers *Snail*, *Slug*, *Twist*, *Sox9*, and *Pax3* was lower or undetectable compared to EGFP⁻ cells, most of these markers were expressed after culture. The expression of neural crest-associated genes was quite similar in EGFP⁺ and EGFP⁻ cells from the WP, whereas in the BM, their expression was significantly higher in EGFP⁺ cells compared to EGFP⁻ cells.

For the EGFP⁺ spheres, although the expression frequencies of neural crest-associated genes differed, the spheres from all three tissues generally expressed most of the neural crest-associated genes. By comparison, CNS neurospheres derived from the E14.5 striatum did not express the neural crest-associated genes *Snail*, *Slug*, *Twist*, *p75*, or *Pax3*. They expressed *sox9* and *sox10* as expected, since these genes are also deeply involved in development of the CNS (Stolt et al., 2003, 2004). *Nkx6.1* is a well-known marker expressed in the

Expression Pattern of Neural Crest-Associated Genes Differs among Tissue Sources

To characterize the mRNA expression profile of neural crest cells derived from each tissue, cells from the adult P0-Cre/Floxed-

ventral half of the neural tube during early development (Jensen et al., 1996). EGFP⁺ cells and spheres did not express *Nkx6.1*, in contrast to its strong expression in embryonic stem cell-derived neurospheres ventralized by the sonic hedgehog protein (Shh)

Table 1. Differentiation Potential of Spheres Derived from DRG, WP, and BM of Adult P0-Cre/Floxed-EGFP Mice

Frequency of Sphere Types (Percent ± SD)							
	NGM	NM	NG	GM	N	M	G	Others
DRG	74.6 ± 1.0	21.8 ± 3.6	2.3 ± 3.2	0	1.0 ± 0.2	0	0	0
WP	7.3 ± 3.6	91.6 ± 3.1	0	0	0	1.1 ± 1.1	0	0
BM	3.3 ± 0.4	15.6 ± 0.8	0.5 ± 0.8	0.8 ± 0.7	7.3 ± 8.5	64.6 ± 11.7	0.7 ± 1.2	7.3 ± 2.6

EGFP+ spheres formed from clonal density cultures of each tissue source were differentiated and subjected to triple immunostaining. The differentiation potential of 100 spheres from each tissue source was individually examined, and each sphere's ability to differentiate into each cell type was determined: N, neurons; G, glial cells; M, myofibroblasts (mean ± SD, n = 3 per group). Spheres derived from the DRG showed a significantly higher frequency of trilineage differentiation potential (N + G + M) than the spheres from other sources (p < 0.05 by Kruskal-Willis test). Of the spheres derived from the BM, 7.3% were negative for all three lineage markers.

(Y.O. and H.O., unpublished data). These results indirectly suggest that the examined cells did not have ventral identities and do not conflict with the fact that they are developmentally derived from the dorsal neural tube, where neural crest cells originate.

EGFP+ Cells of the DRG Strongly Express NCSC Markers in Adult P0-Cre/Floxed-EGFP Mice

To quantify the expression of the NCSC markers Sox10 and p75 in fresh noncultured EGFP+ cells and in spheres cultured for 2 weeks, we performed real-time PCR (Figure 6B). Sox10 and p75 expression was higher in both the noncultured cells and cultured spheres from the DRG compared with those from the WP and BM, suggesting that there is a higher proportion of NCSCs in the DRG. However, since these genes are also expressed in specific neurons and glial cells (Kaplan and Miller, 2000; Paratore et al., 2001), we examined the expression levels of Nestin and Musashi1. Although they are used as markers for undifferentiated cells in the CNS (Lendahl et al., 1990; Sakakibara et al., 1996), they are also expressed in neural crest-derived sphere initiating cells from the heart (Tomita et al., 2005), cornea (Yoshida et al., 2006) and gut (R. Hotta, S.S., and H.O., unpublished data). Since it has been suggested that Nestin and Musashi1 expression may reflect an undifferentiated state (Tomita et al., 2005), their high expression in spheres generated from the DRG also suggests that the DRG contains the highest proportion of NCSCs, and their increased expression after culture suggests that these NCSCs proliferate in culture when spheres are formed.

DISCUSSION

In the present study, by using the double-transgenic mouse strains P0 and Wnt1-Cre/Floxed-EGFP, we examined multiple tissues and organs to map the presence of neural crest-derived cells. We discovered the existence of multipotent NCSCs in the BM and DRG of adult rodents along with the previously reported facial WP. However, analysis of these cells revealed interesting differences that were specific to the tissue source. Careful consideration of these differences will be necessary if these cells are to be recruited for cell transplantation treatments.

Our histological analysis of adult P0 and Wnt1-Cre/Floxed-EGFP mice revealed EGFP+ cells in the BM (Figure 1 and Figure S1). Using flow cytometry, we collected EGFP+ BM cells that proliferated to form spheres (Figure 4). Although the frequency was low, compared with the other tissue sources,

multipotent NCSCs were present in the BM. Clonal spheres with a trilineage differentiation potential into neurons, glial cells, and myofibroblasts were observed, and dissociated cells from these spheres formed secondary spheres (Figure 5, Figures S4 and S5). The presence of NCSCs in the BM is also supported by a recent report using the same P0-Cre reporter mice to demonstrate that a portion of MSCs in the BM of the lower extremities are of neural crest lineage (Takashima et al., 2007). Furthermore, we have unpublished data showing that NCSCs contribute to produce a subpopulation of MSCs in the BM. At the embryonic stage, NCSCs differentiate into many types of neural crest lineage cells, most of which are marked with EGFP in P0 and Wnt1-Cre/Floxed-EGFP mice. We prospectively isolated EGFP+ MSCs from the BM of P0 and Wnt1-Cre mice using flow cytometry and identified that EGFP+ MSCs could generate osteocytes, chondrocytes, and adipocytes (S.M. and Y.M., unpublished data). Together with Nishikawa's report, these findings show that a certain population of MSCs in the BM originates from multipotent NCSCs.

Since a previous report indicated that Wnt1 is expressed in the BM of adult rodents (Almeida et al., 2005), we cannot rule out the possibility that the EGFP+ labeling in the BM of adult Wnt1-Cre/Floxed-EGFP mice was due to the ongoing expression of Wnt1 in the adult BM rather than reflecting a history of Wnt1 expression in the embryonic neural crest lineage. However, we found that the sphere-forming potential and differentiation tendency of EGFP+ cells from the BM of Wnt1-Cre/Floxed-EGFP mice were similar to those from P0-Cre/Floxed-EGFP mice (Figure S4), suggesting the presence of NCSCs among the EGFP+ cells in the BM of adult Wnt1-Cre/Floxed-EGFP mice. The BM stem cells reported in other studies differentiated into neurons and glial cells in vitro and in vivo and also in transplantation experiments (Fernandez et al., 2004; Jiang et al., 2002). Although transdifferentiation or dedifferentiation has been suggested to explain this phenomenon, our results demonstrating the presence of NCSCs in the BM indicate that this differentiation potential may reflect that of NCSCs of the BM. It will be interesting to clarify the relationship between the NCSCs described in the present study and the BM-derived stem cells that are reported to generate neural cells in vitro (Kohyama et al., 2001).

Hematopoiesis is initiated in the yolk sac at the embryonic stage and is successively transferred to the AGM region, fetal liver, and BM with time (Dzierzak and Speck, 2008). Using two independent Cre lines, we detected NCSCs in the AGM region, fetal liver, and BM during a time frame that coincided with the